HHS Public Access

Author manuscript

Nat Microbiol. Author manuscript; available in PMC 2021 August 18.

Published in final edited form as:

Nat Microbiol. 2021 May ; 6(5): 658–671. doi:10.1038/s41564-021-00866-3.

The *Salmonella* Effector Protein SopD targets Rab8 to positively and negatively modulate the inflammatory response

Huan Lian[1,4], **Kun Jiang**[2,4], **Ming Tong**[2,4], **Zhe Chen**[2], **Xiaoyu Liu**[2], **Jorge E. Galán**[1,*], **Xiang Gao**[2,3,*]

[1]Department of Microbial Pathogenesis, Yale University School of Medicine, New Haven, CT 06536, USA

[2]State Key Laboratory of Microbial Technology, Shandong University, 266237 Qingdao, China

[3]School of Life Sciences, Shandong University, 266237 Qingdao, China

Abstract

The food-borne bacterial pathogen *Salmonella* Typhimurium uses a type III protein secretion system to deliver multiple proteins into host cells. These secreted effectors modulate host cell functions and activate specific signalling cascades that result in the production of pro-inflammatory cytokines and intestinal inflammation. Some of the *Salmonella*-encoded effectors counter this inflammatory response and help to preserve host homeostasis. We demonstrate that the *Salmonella* effector protein SopD, which is required for pathogenesis, functions to both activate and inhibit the inflammatory response by targeting the Rab8 GTPase, a negative regulator of inflammation. We show that SopD has GTPase activating protein activity for Rab8, and therefore inhibits this GTPase and stimulates inflammation. We also show that SopD activates Rab8 by displacing it from its cognate guanosine dissociation inhibitor resulting in the stimulation of a signaling cascade that suppresses inflammation. We solved the crystal structure of SopD in association with Rab8 to 2.3 Å resolution, which reveals a unique contact interface underlying these complex interactions. These findings show the remarkable evolution of a bacterial effector protein to exert both agonistic and antagonistic activities toward the same host cellular target to modulate the inflammatory response.

Keywords

bacterial pathogenesis; intestinal inflammation; innate immunity; type III secretion; Rab GTPases; GDI displacement factor; GDF; bacterial effectors; *Salmonella* Typhimurium; Akt signaling

*Corresponding authors: jorge.galan@yale.edu; xgao@email.sdu.edu.cn.

4:These authors contributed equally to this work

CONTRIBUTIONS

H.L. performed all the functional analyses, animal and cell biological experiments, K.J., M.T., and Z.C. carried out the biochemical characterization of SopD and solved its crystal structure bound to Rab8. J.E.G. and X.G. supervised the study, J.E.G. and X.G. wrote the paper with comments from all authors.

COMPETING INTEREST

The authors declare no competing interests.

Salmonella Typhimurium stimulates a potent inflammatory response in the intestinal epithelium through the activities of its type III secretion (TTS) effector proteins SopE, SopE2, and SopB[1-5]. These effectors stimulate these responses independent of innate immune receptors by redundantly targeting the Rho-family GTPase Cdc42[1-5]. The stimulation of Cdc42 results in the activation of its effector p21-activated protein kinase 1 (PAK1), leading to the non-canonical recruitment of Tumor Necrosis Factor receptor-associated factor 6 (TRAF6) and mitogen-activated protein kinase kinase kinase 7 (TAK1), with the subsequent stimulation of NF-κB inflammatory signaling[4]. Additional effector proteins contribute to the enhancement of the inflammatory response by targeting other pro-inflammatory signaling pathways[6-8]. The stimulation of an inflammatory response is central to pathogenicity, allowing *S*. Typhimurium to compete against the resident microbiota and to acquire the nutrients and electron acceptors that sustain its replication[9,10]. Equally important in the *Salmonella*/host interaction, however, is the preservation of host homeostasis. Consequently, in a remarkable "yin and yang", *Salmonella* has evolved a subset of TTS effector proteins that oppose the action of its agonistic effector-protein counterparts. For example, to counter the action of the Rho-family GTPase agonists SopE, SopE2, and SopB, *Salmonella* delivers the effector protein SptP, which exhibits potent GTPase-activating protein (GAP) activity toward the same Rho-family GTPases[11]. Furthermore, to counter the pro-inflammatory effectors that activate NF-κB signaling, *Salmonella* delivers three effector proteins with highly specific protease activity toward the NF-κB transcription factors RelA and RelB[12].

Previous studies have shown that the *Salmonella* TTS effector protein SopD synergizes with other effectors to stimulate inflammation in an animal model of infection[13,14]. However, the mechanism by which this effector carries out this function is unknown. Here we show that SopD exerts its activity by targeting the Rab-family GTPase Rab8, which recent studies have shown to negatively regulate the inflammatory response mediated through Toll-like receptors (TLRs)[15-17]. We found that, through a GAP activity, SopD antagonizes Rab8 thus enhancing the inflammatory response to *Salmonella*. Furthermore, through an additional activity that results in the displacement of Rab8 from its cognate guanosine dissociation inhibitor (GDI), SopD activates this GTPase thus countering the inflammatory response. Therefore, this bifunctional effector protein can both activate and inhibit Rab8-mediated signaling to stimulate and antagonize the inflammatory response induced by *Salmonella*.

Results

SopD is a GAP for Rab8

SopD exhibits significant amino acid sequence similarity to the related *Salmonella* effector protein SopD2[18] (Supplementary Fig. 1), which neutralizes a Rab32-dependent cell intrinsic host defense mechanism by targeting this GTPase with a GAP activity[19]. Of note, a critical arginine residue in SopD2, R315, which is essential for its GAP catalytic activity, is conserved in SopD (Supplementary Fig. 1). However, SopD is unable to complement a Δ*sopD2* mutant for its ability to neutralize the Rab32-pathogen restriction mechanism[19]. Consistent with this finding, we found that SopD did not show any measurable GAP activity toward Rab32 (Fig. 1a). However, we found that of the 24 additional Rab GTPases tested,

SopD showed robust GAP activity only toward Rab8 (Fig. 1b). Like SopD2[19], the GAP activity of SopD was strictly dependent on the R312 residue since the SopD^{R312A} and SopD^{R312K} mutants did not show any measurable GAP activity toward Rab8 (Fig. 1c). We found that SopD was able to form a complex with Rab8 (Fig. 1d) but we were unable to detect a stable complex between Rab8 and SopD2, which also exhibits GAP activity toward Rab8[19] (Extended Data Fig. 1). In addition, transient transfection experiments showed that both the wild type and the catalytic SopD^{R312A} mutant were able to form a complex with Rab8 *in vivo* (Fig. 1e). These results indicate that, like its homolog SopD2, the bacterial effector SopD is also a GAP for a Rab GTPase but with different specificity.

SopD enhances pro-inflammatory signaling by antagonizing Rab8 through its GAP activity

Innate immune receptors are most often “wired” to anti-inflammatory pathways that help the recovery of host homeostasis after an inflammatory response[20-25]. Rab8 has been linked to one such anti-inflammatory pathway downstream of TLRs resulting in the recruitment of Phosphoinositide 3-kinase (PI3-kinase), Akt activation, and the biasing of cytokine production toward an anti-inflammatory program[15-17]. We investigated the potential role of Rab8 in *Salmonella*-induced inflammatory signaling. We examined whether, similar to LPS stimulation[15], Rab8 could also be also recruited to the membrane ruffles stimulated by *S.* Typhimurium by delivering a subset of TTS effector proteins[3,26,27]. We found that Rab8 was robustly recruited to the *Salmonella*-induced membrane ruffles, although recruitment did not require the presence of the effector protein SopD (Extended Data Fig. 2). As Henle 407 cells do not respond to LPS stimulation, these results indicate that, at least in these cells, the *Salmonella*-induced recruitment of Rab8 to membrane ruffles is independent of LPS.

There are two isoforms of Rab8, Rab8a and Rab8b, which exhibit significant (83%) amino-acid sequence identity and are thought to have some overlapping functions[28]. We compared the ability of *S.* Typhimurium to stimulate Akt and NF-κB signaling in wild type and Rab8a-, Rab8b-, and Rab8a/Rab8b-deficient cell lines generated by CRISPR/Cas9-mediated genome editing (Supplementary Fig. 2). Although we detected no differences in NF-κB signaling after *S.* Typhimurium infection, we found significantly reduced levels of Akt phosphorylation in both Raw264.7 and HT29 Rab8a-deficient cell lines (Fig. 2a and Extended Data Fig. 3) despite equal levels of bacterial invasion (Supplementary Fig. 3). Consistent with these observations, in Rab8a-deficient cells infected with *S.* Typhimurium we found significantly reduced mRNA levels for the anti-inflammatory cytokines IL-10 and increased mRNA levels for the pro-inflammatory cytokines IL-1β and Tnfα (Fig. 2b). Although the observed changes were not as pronounced as those observed in the absence of Rab8a, the absence of Rab8b resulted in decreased Akt activation, decreased mRNA levels for the anti-inflammatory cytokine IL-10, and increased levels for the pro-inflammatory cytokines IL-1β and Tnfα after *S.* Typhimurium infection (Fig. 2c and Extended Data Fig. 3). However, the absence of Rab8a and Rab8b resulted in a more pronounced decrease in Akt activation after *S.* Typhimurium infection as well as more significant changes in *IL-10, IL-1β and Tnfα* mRNA levels (Fig. 2d and Extended Data Fig. 3). These results indicate that both, Rab8a and Rab8b redundantly participate in *Salmonella*-induced inflammatory signaling, although Rab8a appears to have a more prominent role.

We then tested the effect of the expression of SopD on LPS-mediated inflammatory signaling. We found that expression of SopD led to significant inhibition of LPS-stimulated Akt activation, although it did not affect NF-κB and MAP kinase signaling (Fig. 2e, Extended Data Fig. 4, and Supplementary Fig. 4). More importantly, expression of SopD resulted in a shift toward a pro-inflammatory cytokine profile with increased production of mRNAs for the pro-inflammatory cytokines Il-1β and Tnfα and decreased production of the mRNA for the anti-inflammatory cytokine IL-10 (Fig. 2f). The SopD-mediated modulation of LPS signaling was strictly dependent on its GAP activity since the expression of the catalytic mutant $SopD^{R312A}$ did not inhibit LPS-mediated signaling (Fig. 2e, 2f, and Extended Data Fig. 4). Taken together, these results indicate that, through its Rab8 GAP activity, SopD has the capacity to enhance *Salmonella*-induced inflammation by interfering with a negative regulatory mechanism linked to a pro-inflammatory signaling pathway.

Previous studies have shown that Rab8-dependent LPS-mediated Akt activation and the resulting anti-inflammatory response requires PI3 kinase[15-17]. In addition, *S.* Typhimurium has been shown to activate Akt by stimulating phosphoinositide fluxes through the delivery of its TTSS effector protein SopB[29,30]. We found that, similar to LPS stimulation, the *S.* Typhimurium-induced Akt activation in both Raw264.7 macrophage and HT29 also required PI3 kinase (Extended Data Fig. 5a). The addition of increasing concentrations of wortmannin, a specific PI3 kinase inhibitor, resulted in a progressive inhibition of *Salmonella*-induced Akt activation. Importantly, the addition of the PI3 kinase inhibitor resulted in increased mRNA levels for the pro-inflammatory cytokines Il-1β and Tnfα and reduced mRNA levels for the anti-inflammatory cytokine IL-10 (Extended Data Fig. 5b).

Taken together, these results implicate both, Rab8a and Rab8b as well as PI3 kinase in the negative modulation of the inflammatory response to *Salmonella* Typhimurium. Importantly, these results suggest a mechanism by which the effector protein SopD through its GAP activity enhances the inflammatory response to *Salmonella* by inhibiting Rab8.

The crystal structure of SopD in complex with Rab8 reveals a functional interface that suggests the presence of an additional activity

To better define their functional interface, we solved the crystal structure of SopD in complex with Rab8a at 2.3 Å resolution. The complex is formed by one molecule each of SopD and Rab8 and is arranged in a V-shaped architecture, with each of the molecules forming one leg of the V (Fig. 3a and Supplementary Fig. 5). The interface between SopD and Rab8 buries ~1000 $Å^2$ surface area. Close inspection of this interface revealed structural elements in Rab8 that contain Rab-family- (RabF) and Rab-subfamily-specific (RabSF) motifs [31,32], which form a “hand-in-hand” interface with the α11 helix, β4/β5 anti-parallel sheets, as well as loops L_A, L_B and L_C in SopD (Fig. 3a, 3b, and Supplementary Fig. 5). SopD engages the RabF motif through hydrophobic interactions between its residues V237 and A242 and the Rab8 residues I43, F45, and W62. In addition, polar interactions between K58, T74, and R79 in Rab8 and Q107, S138, E240, Y278 and E293 in SopD, as well as two water-mediated hydrogen bonds between Q60 in Rab8 and K285 and D289 in SopD further stabilize the complex (Fig. 3b and 3c). Additional interactions involve residues within the RabSF motif in Rab8 (Y5, Y7 and L177) and E293, V290 and F287 in SopD and

hydrophobic interactions between A76 in the switch II region of Rab8 and M139 in SopD, M82 in Rab8 and M286 in SopD, as well as one direct hydrogen bond between K46 in Rab8 and Q238 in SopD (Fig. 3b and 3c).

Surprisingly and contrary to what its GAP activity would predict, the Rab8/SopD interface does not position the catalytic Arg312 of SopD in close proximity to the nucleotide-binding pocket of Rab8 (Fig. 3a). Rather, the arrangement of SopD in the complex positions its Arg312 catalytic residue on the opposite side of its Rab8-interacting surface. Furthermore, although a clear electron density for GDP and Mg^{2+} was apparent, no electron density corresponding to ALF_3 could be discerned in the structure, despite its presence in the crystallization buffer (Fig. 3a and Supplementary Fig. 6). This is consistent with the observation that SopD was able to form a complex with GDP-loaded Rab8 (Extended Data Fig. 6).

The overall structure of SopD in the complex is virtually identical to its previously determined apo-structure[33], with a root-mean-squared deviation (rmsd) of 0.499 Å over 255 Cα atoms (Supplementary Fig. 7). Structural alignment of Rab8 as it appears in complex with SopD with either the GDP-bound Rab8 from the Rab8-Rabin8 complex (RCSB ID 4LHY) or GDP-bound inactive Rab8 (RCSB ID 4LHW)[34] reveals marked conformational change in the switch I and II as well as the RabSF1 regions of Rab8 that occur upon SopD binding (Fig. 3d and Supplementary Fig. 8). These conformational changes position residues T74, R79, Y5, and K58 in Rab8 to engage in critical interactions with residues Q107, Y278, E240, and E293 in SopD.

To examine the potential functional significance of the observed SopD/Rab8 interface, we introduced structurally-guided mutations in SopD residues (Q107L/Q238L, S138A/Y278A and E293A) predicted to play a role in the formation of the complex. We then purified the resulting mutant proteins and examined their ability to form a complex with Rab8 *in vitro*. We found that the introduction of one of the mutations (E293A) completely abolished the ability of SopD to form a complex with Rab8 *in vitro* demonstrating the importance of this interface in the formation of the SopD/Rab8 complex (Fig. 3e and Extended Data Fig. 7). Consistent with this finding, introducing the E293A mutation also disrupted the ability of SopD to interact with Rab8 in transient transfection experiments in cultured cells (Fig. 3f and Extended Data Fig. 8). Of note, critical SopD residues necessary for its interaction with Rab8 (e. g E293) are absent from SopD2 (Supplementary Fig. 1), which is consistent with the inability of SopD2 to form a complex with Rab8 (Extended Data Fig. 2). These results indicate that the identified interface is critical for the formation of the Rab8/SopD complex. We also examined the GAP activity of different SopD mutants, including the mutant (E293A) that disrupted its ability to form a complex with Rab8. We found that none of the mutations affected the GAP activity of this effector protein (Fig. 3g). Taken together, these results indicate that the interface captured in the SopD/Rab8 complex is unrelated to the GAP activity of SopD and suggest the presence of an additional function associated with this effector protein.

SopD activates Rab8 through a functional interface unrelated to its GAP activity

The molecular interface between SopD and Rab8 suggested the presence of a potential additional function in this effector protein independent of its GAP activity. To investigate this hypothesis, we examined the levels of Rab8 activation in HEK-293T cells that had been transiently transfected with plasmids expressing wild type SopD, its GAP catalytic mutant ($SopD^{R312A}$), a mutant that disrupts its interaction with Rab8 ($SopD^{E293A}$), or a mutant defective for both activities ($SopD^{R312A/E293A}$). Alternatively, we co-transfected the same plasmids along with a plasmid expressing Rabin 8, an exchange factor for Rab8[35]. To assess the levels of Rab8 GTP-loading, a measure of its activation, we took advantage of a previous observation indicating that Mical L2, an effector of various Rab GTPases, can selectively bind to GTP loaded Rab8[36]. We found that the expression of wild type SopD did not significantly alter the levels of GTP-loaded Rab8 in comparison to controls (Fig. 4a and Supplementary Fig. 9a). However, expression of $SopD^{R312A}$ resulted in an increased level of GTP-loaded Rab8, while expression of $SopD^{E293A}$ led to a reduction in the levels of activated Rab8 (Fig. 4a and Supplementary Fig. 9a). The observed effects were also apparent when the mutant proteins were co-expressed with Rabin 8 (Fig. 4b and Supplementary Fig. 9b). Expression of the SopD mutant defective in both activities ($SopD^{R312A/E293A}$) did not alter the levels of GTP-loaded Rab8 in comparison to controls (Fig. 4a and 4b and Supplementary Fig. 9a and 9b). Taken together, these results are consistent with the notion that, in addition to the negative regulatory GAP activity, SopD has a Rab8 stimulatory activity that depends on the functional interface identified through the structural analysis.

The observation that SopD possesses a Rab8-activating function prompted us to investigate whether SopD exhibited guanine nucleotide exchange factor (GEF) activity. We detected no GEF activity in SopD, although as predicted[35], we detected robust exchange activity of the Rab8 exchange factor Rabin 8 (Extended Data Fig. 9). Therefore, SopD must activate Rab8 by an alternative mechanism. After their activation and membrane targeting, small GTPases are extracted from the plasma membrane and maintained in a cytosolic soluble form by cognate regulatory proteins known as guanine dissociation inhibitors (GDI). These regulators play a critical role in the functional recycling of Rab GTPases[37,38]. Upon reception of an appropriate signal, the GDP-Rab GTPases must be released from their GDIs prior to their activation and membrane targeting[39-41]. Therefore, we examined whether SopD could displace Rab8 from its cognate GDI. We expressed in cultured HEK-293T cells epitope-tagged versions of Rab8 and GDI2 and examined their interaction by co-immunoprecipitation in the presence of purified wild type SopD, its GAP defective mutant ($SopD^{R312A}$), or a mutant that disrupts its interaction with Rab8 ($SopD^{E293A}$). We found that the addition of increasing amounts of purified wild-type SopD or its GAP-defective mutant ($SopD^{R312A}$) resulted in a significant reduction on the amount of Rab8 bound to GDI2 (Fig. 4c and 4d). In contrast, the addition of purified $SopD^{E293A}$ or SopD2, which are unable to form a complex with Rab8, did not affect the levels of Rab8 bound to GDI2 (Fig. 4d). We also expressed in HEK-293T cells the same SopD mutants along with the epitope-tagged version of Rab8 and GDI2 and examined the levels of Rab8 bound to GDI2 by a co-immunoprecipitation assay. We found that the levels of Rab8 bound to GDI2 significantly decreased upon expression of wild type SopD or its GAP catalytic mutant ($SopD^{R312A}$) but remained unchanged when co-expressed with $SopD^{E293A}$ (Fig. 4e and Supplementary Fig.

9c). Taken together, these results indicate that SopD has the ability to stimulate Rab8 by promoting its dissociation from its cognate GDI.

Mechanistic insight for the Rab8-activating function of SopD inferred from the crystal structure of the SopD/Rab8 complex

To gain insight into the potential mechanism by which SopD displaces GDI, we compared the atomic interface between SopD and Rab8 with the interface between the yeast Rab GTPase Ypt1 and its GDI (RCSB ID 2BCG). Comparison of the two structures shows that while there is significant overlap between the two interfaces on the "open end" of the V-shaped complex, this is not the case on the "closed end" of the complex (Fig. 5a and 5b). On this end there are no significant interactions between Ypt1 and its GDI but SopD engages Rab8 in unique interactions. These interactions include the SF (Y5, Y7 and L177) and F2 regions (K58 and Q60) of Rab8 as well as less conserved amino acid residues such as K46 and M82 (Figure 5b). These interactions may provide the structural bases for the initial engagement of GDI-bound Rab8 by SopD, which would ultimately lead to conformational changes that destabilize the Rab8-GDI complex. In support of this notion, a mutation of a critical residue in SopD ($SopD^{E293A}$), which specifically interacts with Y5 and K58 in Rab8, effectively prevented the ability of SopD to displace GDI from Rab8 (Fig. 4d and 4e). We propose that the initial engagement of the close end of the Rab8-GDI complex by SopD leads to the destabilization of critical Rab8-GDI interactions that maintain the stability of the complex exemplified by a network of hydrogen-bonds between D44 in Ypt1 and R106, Y107, R248 and R445 in the GDI (Fig. 5c). The SopD-induced destabilization of this network would lead to an outward movement of ~4Å of the GDI-binding platform (centered in the G42 residue in the case of Ypt1). These conformational changes would also lead to repulsive interactions between I252 in the GDI and G42 and D44 in Rab8 (Fig. 5c). Furthermore, the switch II region of Ypt1, which interacts strongly with GDI, would be also disrupted by SopD binding (Fig. 5d). These conformational changes would result in a ~6Å inward movement of switch II thus destabilizing critical hydrophobic interactions between this region (e. g. residue A65 in Rab8) and a hydrophobic patch in GDI formed by A247, A251 and I252 (Fig. 5d). The SopD-induced conformational changes in switch II would also destabilize additional critical Rab8-GDI interactions exemplified by those between residues T72 and S75 in Ypt1 (or the corresponding T72 and T75 residues in Rab8) and Y44 and Q244 in GDI (Fig. 5d). In summary, we propose a model in which by engaging Rab8 residues not involved in its interaction with GDI, SopD triggers conformational changes in critical regions of Rab8, in particular switch II, resulting in the destabilization of the Rab8/GDI complex and the subsequent release of GDI.

SopD positively and negatively modulates *S.* Typhimurium-induced inflammatory signaling through its independent Rab8-modulating activities

The discovery that SopD has the capacity to both, activate and inhibit Rab8, prompted us to investigate the potential role of these activities in the context of *Salmonella* infection. We infected Raw264.7 macrophages and HT29 intestinal epithelial cells with wild-type *S.* Typhimurium or its isogenic mutants Δ*sopD*, $sopD^{R312A}$, or $sopD^{E293A}$. To facilitate interpretation of the results, we also introduced a Δ*sopD2* deletion as this effector protein also exhibits Rab8 GAP activity, although it lacks Rab8-activating activity (see above). We

found that infection of either cell line with *S*. Typhimurium expressing the GAP-defective SopD^{R312A} mutant resulted in significantly higher Akt activation in comparison to cells infected with wild type (Fig. 6a and Supplementary Fig. 10). In contrast, cells infected with *S*. Typhimurium expressing SopD^{E293A}, which is defective for Rab8 activation, resulted in a decrease in Akt activation (Fig. 6a and Supplementary Fig. 10). Consistent with these observations, cells infected with the *S*. Typhimurium Δ*sopD2 sopD*^{R312A} mutant showed increased levels of anti-inflammatory cytokines IL-10 and decreased levels of the pro-inflammatory cytokines IL-1β and Tnfα (Fig. 6b and Extended Data Fig. 10). In contrast, cells infected with *S*. Typhimurium expressing the *sopD*^{E293A} allele showed the reversed pattern: decreased levels of IL-10 and increased levels of Il-1β and Tnfα (Fig. 6b and Extended Data Fig. 10). This is consistent with the notion that SopD has the capacity to both enhance and suppress the inflammatory response to *S*. Typhimurium during infection.

We also compared the intestinal inflammatory response of mice infected with *S*. Typhimurium Δ*sopD2* strain expressing either the SopD^{R312A} GAP-deficient mutant, or the SopD^{E293A} mutant deficient for Rab8 activation. We found significantly lower mRNA levels for the pro-inflammatory cytokines IL-1β and Tnfα in the intestines of mice infected with *S*. Typhimurium strain expressing the *sopD*^{R312A} GAP-deficient allele in comparison to mice expressing wild-type SopD (Fig. 6c). The difference was more pronounced when compared to the levels found in the intestines of mice infected with the *S*. Typhimurium strain expressing the SopD^{E293A} mutant deficient for Rab8 activation, which showed increased levels of pro-inflammatory cytokine mRNAs even when compared to mice infected with wild type (Fig. 6c). Taken together, these results indicate that the effector protein SopD through its contrasting Rab8-modulating activities has the capacity to enhance and suppress the inflammatory response to *S*. Typhimurium.

Discussion

In this study we describe a remarkable *S*. Typhimurium TTSS effector protein that can stimulate both, pro- and anti-inflammatory signaling. This bifunctional effector accomplishes this feat by targeting an anti-inflammatory pathway orchestrated by the Rab8 GTPase[15-17]. Through agonistic and antagonistic activities toward Rab8, SopD can alternatively suppress or enhance the inflammatory response to *Salmonella* (Fig. 6d). Rab8 is linked to anti-inflammatory signaling emanating from TLR4[15-17]. Since *Salmonella* LPS is a potent activator of TLR4, it is possible that SopD exerts its effect in the context of LPS-mediated signaling. However, we have also shown that *S*. Typhimurium can trigger a SPI-T3SS- and Rab8-dependent Akt-mediated anti-inflammatory signaling in cultured intestinal epithelial cells that do not respond to LPS. These findings therefore indicate that by inhibiting Rab8 through its GAP activity, SopD can exert its pro-inflammatory effect in the context of both, LPS and *Salmonella*-induced anti-inflammatory signaling.

We have also shown that SopD can also stimulate Rab8-dependent anti-inflammatory signaling by displacing Rab8 from its cognate GDI. Through structure/function analyses, we have shown that SopD function resembles that of eukaryotic GDI displacement factors (GDFs), which release Rab GTPases from their GDIs thus allowing their recycling to the plasma membrane where they can be activated by their cognate GEFs[40,41].

The opposing activities of SopD raise the question of how these activities are coordinated in time (Fig. 6d). As pro-inflammatory signaling precedes the anti-inflammatory response, it follows that the GAP activity of SopD should precede its Rab8 stimulatory activity. In fact, T3SS-mediated pro-inflammatory signaling occurs immediately after infection therefore it would be expected that the SopD pro-inflammatory activity through its GAP enzymatic function should be exerted very early in infection, along with that of the Cdc42 agonists SopE, SopE2 and SopB. The cell homeostasis recovery process would then be initiated by the Rab8-agonist activity of SopD, along with the activities of other T3SS effectors such as SptP, which antagonizes Cdc42 [11], SopB, which activates Akt [29], as well PipA, GogA, and GtgA, which directly target the NF-κB transcription factors for degradation[12]. In all cases, substrate availability (i. e. GTP loaded or GDI-bound Rab8) will ultimately define which of the SopD activities are exerted at a given time during infection.

In summary, we have described here a bifunctional bacterial effector protein that can exert agonistic and antagonistic activities toward a single target, Rab8, and thus modulate the inflammatory response. This is a remarkable example of a bacterial determinant shaped by long-standing host-pathogen interactions aimed at facilitating pathogen replication while preserving host homeostasis.

Methods

Bacterial strains

All *Salmonella* Typhimurium strains described are listed in Supplementary Table 1, were derived from the wild-type isolate SL1344[42], and were constructed using standard recombinant DNA and allelic exchange procedures as previously described[43] using the *E. coli* β-2163 Δ*nic35* as the conjugative donor strain[44]. Strains were routinely cultured in LB broth at 37°C.

Cell lines

HEK-293T, HT29 and Raw264.7 cells were obtained from ATCC. Cells were cultured in Dulbecco's modified Eagle medium (DMEM, GIBCO) supplemented with 10% Fetal Bovine Serum (FBS) at 37°C with 5% CO_2 in a humidified incubator. All cell lines were routinely tested for mycoplasma contamination using a Mycoplasma Detection Kit (Southern Biotech, Cat# 13100-01).

Plasmid construction

For recombinant protein expression in *E. coli* the full-length *sopD*, *sopD2* and the truncated *sopD*$^{34\text{-}end}$ lacking its type III secretion signal were cloned into the pET15b expression vector with an N-terminal His tag. Full-length *rab8a* and truncated *rab8a*$^{1\text{-}183}$ were cloned into the pET15b vector (Novagen), introducing an N-terminal 6-His tag, or into the pET28a vector, introducing an N-terminal 6×His-SUMO (small ubiquitin-like motif) tag. Expression vectors for all other human Rab GTPases used in this study were constructed by cloning the different Rab GTPases into the pET15b vector. For expression in mammalian cells, the *sopD* and *sopD2* genes were amplified from *S.* Typhimurium SL1344 and cloned into the pRK-5 or pSin3xHA vectors to generate N-terminal FLAG- or HA-tagged versions of these

proteins, respectively. The *rab8* gene was cloned into the pRK-5 vector introducing an N-terminal Flag or GFP tag. The GDI2 cDNA was amplified from cDNA obtained from HEK-293T cells by reverse transcription,or from a plasmid encoding this gene (pCellFree_G03 GDI2, Addgene) and cloned into pRK-5 resulting in N-terminal HA- or FLAG-tagged versions of this protein. A cDNA encoding $Rabin8_{153-237}$ was amplified from HEK-293T cells and cloned into the pET28a vector with an N-terminal 6×His-SUMO tag or from a plasmid encoding full-length Rabin8 (FLAG-Rabin8, Addgene). All truncations and point mutations were generated by the Gibson assembly strategy[45]. All plasmids were verified by DNA sequencing.

Protein expression and purification

E. coli B21 (DE3) carrying plasmids expressing the different His-tagged SopD constructs were grown in lysogeny broth (LB) medium to an OD600 of 0.8, expression of the different proteins was induced by addition of 0.4 mM isopropyl-β-D-thiogalactopyranoside (IPTG), and cultures were further incubated for 12 hs at 25°C. Bacterial cells were harvested by centrifugation and the pellets were resuspended in lysis buffer [20 mM Tris–HCl (pH 8.0) 150 mM NaCl]. Bacterial cells were lysed with a high pressure cell crusher (Union-Biotech co LTD), the supernatants were collected, run through a Ni-NTA agarose resin (Qiagen), washed with 20 mM Tris-HCl (pH 8.0), 150 mM NaCl, 20 mM imidazole, and proteins were eluted in the same buffer with 300 mM imidazole. Proteins were further purified by HiTrap Q HP ion-exchange and Superdex 200 Increase 10/300 GL (GE Healthcare Life Sciences) chromatography. Full-length His-tagged Rab8a and truncated $Rab8a^{1-183}$ were expressed in *E. coli* BL21(DE3) grown in Terrific broth (TB) at 25°C for 48 hs. The different Rab proteins were purified using Ni-NTA agarose resin (Qiagen) as described previously[19], the SUMO tag was removed with homemade His-tagged ULPI protease at room temperature for 2 hs, and proteins were further purified by Superdex 200 gel filtration chromatography.

To prepare SopD (or its mutants) in complex with Rab8a, purified His-SopD (or its mutants) was incubated with $Rab8a^{1-183}$ at a molar ratio of 1:3 at room temperature for 2 hs in a buffer containing 20 mM Tris (pH 7.5), 150 mM NaCl, 2 mM $MgCl_2$, 1 μm GTPγS (or 20 mM NaF, 0.2 mM $AlCl_3$, 1 μm GDP), and 3 mM DTT. The stable complex was obtained after Superdex 75 Increase 10/300 GL or Superdex 200 Increase 10/300 GL column chromatography. As negative controls, the respective monomers were analyzed by gel filtration chromatography in an identical manner.

Protein crystallization and structure determination

The crystals of the SopD/Rab8 complex were grown at 18°C using the hanging-drop vapor diffusion method by mixing the protein and well solution at a 1:1 ratio. Crystals were obtained under 0.05 M Sodium cacodylate trihydrate (pH 6.5), 0.2 M $MgCl_2$, 11.5% PEG4000. The crystals of the SopD/Rab8 complex were soaked with 30% glycerol then flash-cooled in liquid nitrogen. Diffraction data were collected on the BL17U1 beamline at Shanghai Synchrotron Radiation Facility (Shanghai, China) and processed with the XDS package[46]. Phase of this structure was determined by molecular replacement using SopD (PDB code: 5CPC) and Rab8 (PDB code: 4LHW) structures as searching models and the Phaser program in CCP4 [47]. The model was manually built with Coot [48]. All the structures

were refined with PHENIX [49], and manual modeling was performed between refinement cycles. Statistics of data collection and refinement are summarized in Supplementary Table 2. All the structures were prepared for graphic display using PyMOL [50].

Co-immunoprecipitation and immunoblotting analyses

HEK-293T cells were transiently transfected with plasmid DNAs encoding the indicated proteins or empty vector (as indicated in the figure legends) using the Lipofectamine 2000 reagent (Invitrogen) following the manufacturer's instruction. Twenty-four or forty-eight hours after transfection, ~1× 10^7 cells were collected and lysed in 1 ml lysis buffer [20 mM Tris-HCl (pH7.4), 150 mM NaCl, 1 mM EDTA, 1% NP-40] for 15 min on ice. The cell lysates were centrifuged at 14000 rpm for 15 min at 4°C, supernatants were collected, mixed with anti-Flag M2 agarose affinity gel (Sigma), incubated for 3 hs at 4 °C, and beads were washed four times with cell lysis buffer containing 0.5 M NaCl. Protein bound to the resin was eluted by adding 3 × Flag peptide (200 ng μl^{-1}) (MedChem Express) for 30 min at 4°C and the eluates were analyzed by western blotting. Alternatively, the beads were mixed with sample buffer prior to their separation on 10% SDS-PAGE. Proteins were transferred onto Polyvinylidene fluoride (PVDF, Millipore) or nitrocellulose membranes and processed for immunoblot analyses with the different antibodies as indicated in the figure legends. Blots were treated with the indicated primary antibodies (see figure legends) and with either HRP-coupled or DyLight conjugated secondary antibodies [emission 800 nm (ThermoFisher Scientific, Waltham, MA, USA). Blots were finally developed with M5 Hiper ECL Western HRP Substrate (Mei5 Biotechnology) or visualized on a LI-COR Odyssey imaging system (Lincoln, NE, USA). When required, the intensity of the bands was quantified with the Odyssey v3.0 software package (LI-COR).

For competition binding assays, different concentrations of SopD or its mutants were added to the indicated cell lysates prior to the addition of the anti-Flag M2 agarose affinity gel and samples were processed for co-immunoprecipitation as indicated above.

GAP Assay

The intrinsic and GAP-accelerated GTP hydrolysis of the different GTPases were measured with the High Throughput colorimetric GTPase assay kit (Innova Biosciences). Briefly, purified Rab GTPases (15 μM) were mixed with the different SopD preparations (1.5 μM) in a buffer containing 50 mM Tris-HCl (pH 7.5), 150 mM NaCl, 2.5 mM $MgCl_2$, and 0.5 mM GTP. The mixture was dispensed onto 96-well microplates and incubated for 2 hs at room temperature. The release of inorganic phosphate was quantified by measuring the absorbance at 635 nm of the different samples on a microplate reader (Tecan).

GEF Assay

The GEF activity of SopD toward Rab8a was measured as previously described[51]. Briefly, Rab8a was loaded with mant-GDP by incubation with a 20-fold molar excess of mant-GDP over the GTPase and a 10-fold molar excess of EDTA over $MgCl_2$ for 1.5 hs at room temperature. GDP binding was stabilized by adding $MgCl_2$ to twice the EDTA-concentration. The buffer was subsequently exchanged with 20 mM Tris-HCl (pH 7.5), 150 mM NaCl, 2 mM $MgCl_2$ by gel-filtration chromatography. Mant-GDP-bound $Rab8a^{1\text{-}183}$ (2

μM) was incubated with 0.4 μM of Rabin8$^{153-237}$ proteins (or 2 μM SopD/SopD^{R312A}/SopD^{E293A}) in the presence of 5 μM of GTPγS in the reaction buffer [20 mM Tris-HCl (pH 7.5), 150 mM NaCl, and 2 mM $MgCl_2$]. Fluorescence of mant-GDP was excited directly at 360 nm and detected at 450 nm. Fluorescence emission was read out every 10 seconds for a total of 1200 seconds.

Rab8 activation assay

The levels of GTP-loaded Rab8, a measure of its activation, were determined using a previously developed assay based on the ability of Mical-L2, an effector of various Rab GTPases, to selectively bind GTP loaded Rab8[36]. GST-Mical-L2 was purified by affinity chromatography using Glutathione Sepharose 4B beads following standard procedures. Plasmids encoding GFP-tagged Rab8A, Flag-tagged Rabin8, along with HA- or Flag-tagged SopD or its mutants were co-transfected into HEK-293T cells. Twenty-four hours after transfection, cells were lysed in lysis buffer [20 mM Tris-HCl (pH7.4), 150 mM NaCl, 1 mM EDTA, 1% NP-40] for 15 min on ice. The cell lysates were centrifuged at 14000 rpm for 15 min at 4°C, supernatants were collected and incubated with 1 μg of GST-tagged C-terminal fragment Mical-L2 for 1 hour at 4°C. The beads were then washed with lysis buffer, and the samples were analyzed by immunoblotting with the appropriate antibodies.

S. Typhimurium cell infection

S. Typhimurium was grown overnight in LB, cultures were diluted 1/20 into fresh LB containing 0.3 M NaCl and further grown to an OD_{600} of 0.9. Raw264.7 or HT29 cells were then infected with the indicated *S*. Typhimurium strains at the multiplicities of infection (MOI) indicated in the figure legends. Cells were then washed three times with Hank's balanced salt solution (HBSS) and treated with gentamicin (100 μg/ml) for 1 hour to kill extra-cellular bacteria. Cells were then washed and cultured in medium with low concentration gentamicin (10 μg/ml) for the times indicated in the figure legends.

S. Typhimurium cell invasion assay

The ability of *S*. Typhimurium to invade cultured cells was measured by the gentamicin protection assay as previously described[52].

Generation of CRISPR/Cas9 edited cell lines

Generation of CRISPR/Cas9 edited cell lines was carried out as described previously [53] following standard protocols [54]. Briefly, double-stranded oligonucleotides corresponding to the target sequences were cloned into the lenti-CRISPR-V2 vector and co-transfected with the packaging plasmids into HEK-293T cells. Two days after transfection, the viruses were harvested and used to infect Raw264.7 or HT29 cells. The virally transduced cells were selected in culture media containing puromycin for 5 days and the isolated clones were screened by PCR and sequencing to identify knockout cells. The nucleotide sequence of the guide RNAs and primers used to construct the different cell lines are listed in Supplementary Table 3.

Generation of stable cell lines

Stable Raw264.7 cells expressing HA-tagged SopD or its different mutants were generated through viral transduction and puromycin selection. Briefly, transducing viruses were produced by co-transfecting plasmids encoding HA-tagged SopD or its mutants along with the packaging plasmids into HEK-293T cells. Two days after transfection, the viruses were harvested and used to infect Raw264.7 cells. The infected cells were selected with puromycin for at least 5 days and resistant cells were tested for the expression of SopD or its mutants.

Quantitative PCR

Quantitative PCR of mRNA in cultured cells and mouse tissues was performed as described previously[12]. Briefly, ceca from infected animals removed, cut open, wash extensively with PBS and epithelial cells were collected into a centrifuge tube by scraping the tissue with a glass slide. Total RNA from cultured cells or mouse ceca were isolated using TRIzol reagent (Invitrogen) according to the manufacture's protocol, and was reversed transcribed with iScript reverse transcriptase (Bio-Rad). Quantitative PCR was performed using iTaq SYBR Green Supermix (Bio-Rad) in an iCycler real time PCR machine (Bio-Rad). Data shown are the relative abundance of the indicated mRNAs normalized to that of GAPDH. The primers used for the quantitative PCR are listed in Supplementary Table 4.

Cytokine quantification

Raw264.7 cells were infected with different bacterial strains as indicated in the figure legends for 18 hours. The levels of the cytokines IL-10, IL-1β, and TNFα in the culture media of infected cells were measured by ELISA as indicated by the manufacturer (BioLegend cat# 431417, 432604, and 430907, respectively). The actual concentration of the cytokines was determined using a standard curve (concentration range for the standards: IL-10 and TNFα: 15.6 pg/ml-1000 pg/ml; IL-1β: 31.3 pg/ml-2000 pg/ml).

Mouse infections

All animal experiments were conducted according to protocols approved by Yale University's Institutional Animal Care and Use Committee (IACUC) under protocol number 2019-07858. Eight to twelve-week old C57BL/6 male and female mice carrying a wild type allele of *Nramp1* (*Slc11a1*) [55] were orally infected by stomach gavage with the different *S.* Typhimurium strains as previously described [12]. Four days after infection, mice were sacrificed, ceca removed and processed for qPCR analysis as described above. The number of animals was determined based on prior experience conducting similar experiments and the experimenter was not blinded to the different conditions. Animals were housed in a specific pathogen free animal facility at Yale University in an ambient 21–22 °C temperature room with standard 12:12 h light:dark cycle (lights on 07:00–19:00) with chow and water provided ad libitum.

Statistical analysis

Experiments were performed at least three times independently. Data are shown as arithmetic means ± SD, unless otherwise stated. All statistical data were calculated using

GraphPad Prism version 8.0 (GraphPad Software, San Diego, CA). For comparisons of the means of two groups, unpaired two-sided *t* test was used. For comparisons of multiple groups with a control group, one-way ANOVA method was used, while a two-way ANOVA was used for multiple comparisons. Significance of mean comparison is annotated as follow: ns, not significant; * $P<0.05$; ** $P<0.01$; *** $P<0.001$. A P value of < 0.05 was considered to be statistically significant.

DATA AND CODE AVAILABILITY

The atomic coordinates and structure factors generated in this study have been deposited in the Protein Data Bank with the accession codes 7BWT.

Extended Data

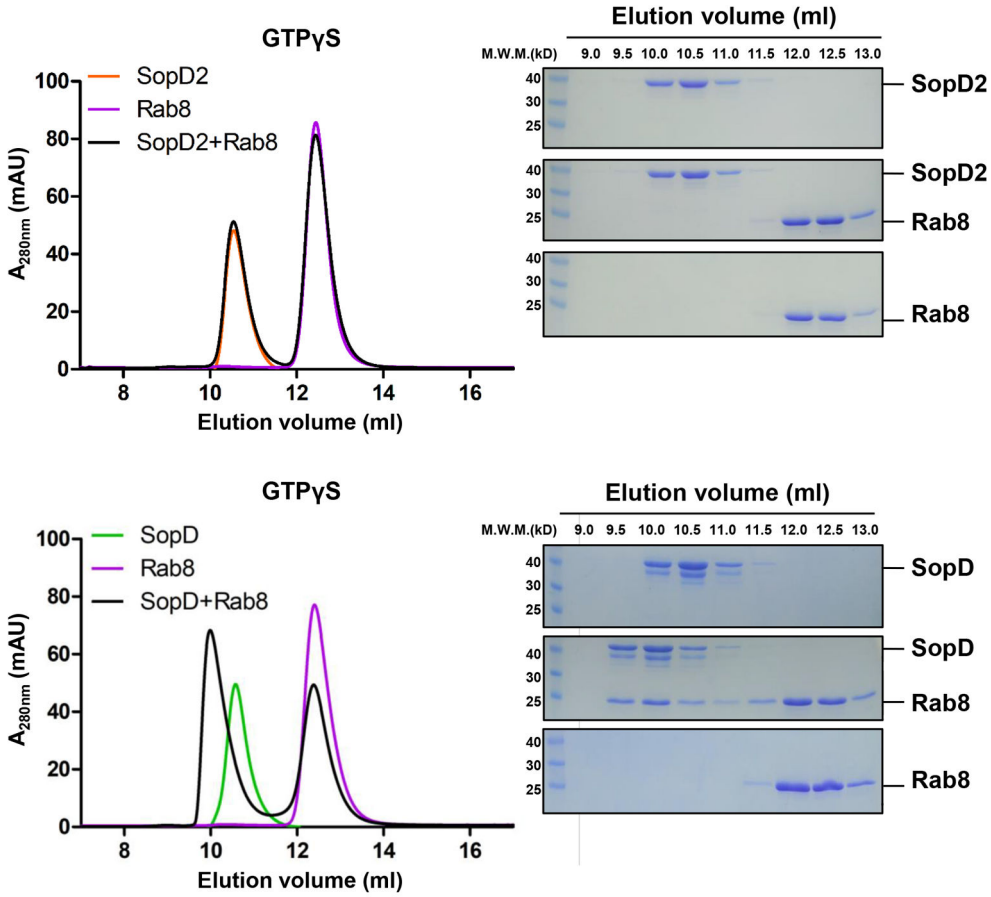

Extended Data Fig. 1. Size-exclusion chromatography analyses of Rab8 in the presence of SopD or SopD2.

Purified $Rab8^{1-183}$ preloaded with GTPγS was incubated with purified SopD or SopD2 and subjected to size-exclusion chromatography in a Superdex 75 increase column. Elution profiles along with SDS-PAGE analyses of the elution fractions are shown. This experiment was conducted at least three times with equivalent results.

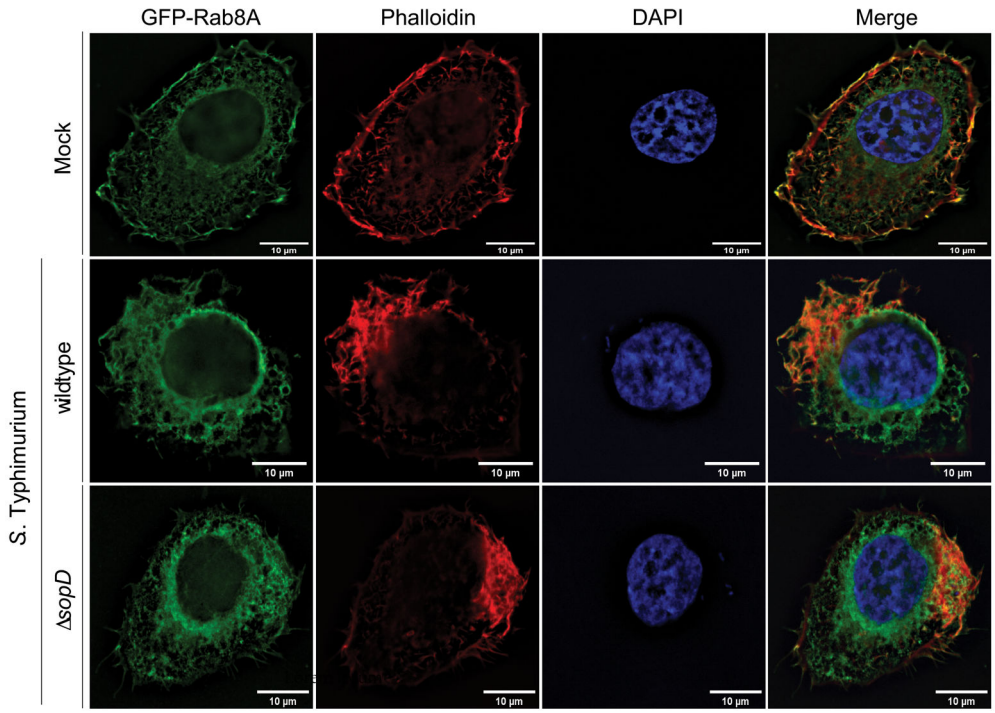

Extended Data Fig. 2. Rab8 is recruited to the *Salmonella*-induced membrane ruffles.
Henle-407 cells were transiently transfected with a plasmid expressing GFP-Rab8A and subsequently infected with wild-type *S.* Typhimurium, its Δ*sopD* isogeneic mutant, or left uninfected (mock). Fifteen minutes after infection, cells were fixed and stained with anti-GFP antibody, to visualize Rab8A (green), rhodamine-labeled Phalloidin, to visualize the actin cytoskeleton (red), and 4’,6-diamidino-2-phenylindole (DAPI) to visualize nuclear and bacteria DNA (blue). Scale bar: 10 μm. This experiment was conducted at least three times with equivalent results.

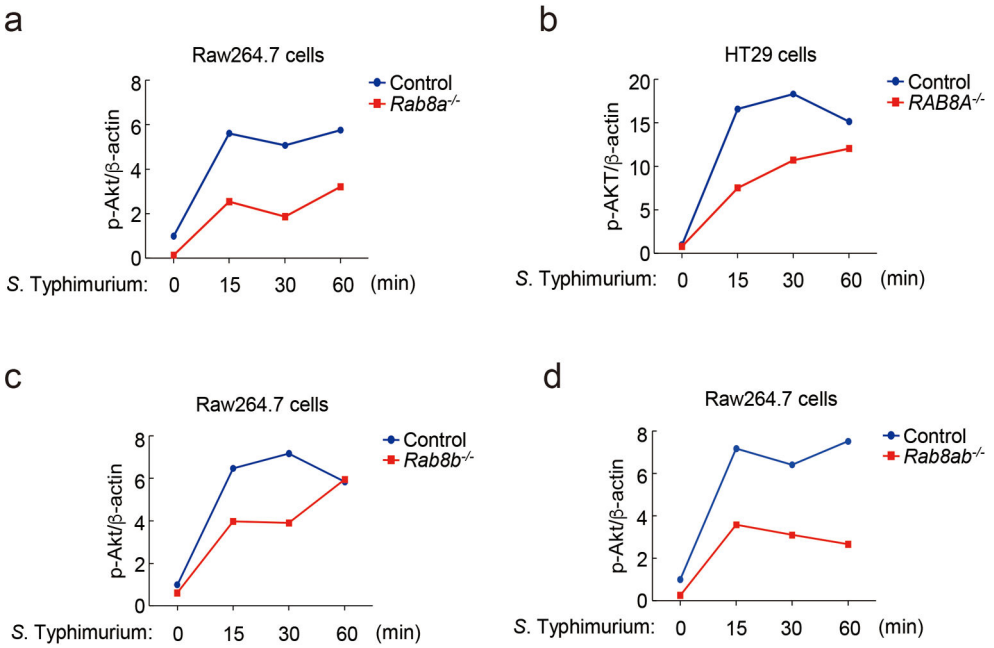

Extended Data Fig. 3. Rab8 negatively modulates *Salmonella*-induced pro-inflammatory signaling.

Effects of Rab8a (**a** and **b**), Rab8b (**c**), or Rab8ab (**d**) deficiency on *S.* Typhimurium-induced AKT activation. Control or deficient Raw264.7 or HT29 (as indicated) cells were infected with wild-type *S.* Typhimurium with a multiplicity of infection of 2 and 10, respectively, and at the indicated times after infection, the levels of phosphorylated Akt were determined by immunoblotting analyses as indicated in Materials and Methods. Values are normalized to the β-actin signal, which served as a loading control. The western blots for this experiment are shown in Fig. 2.

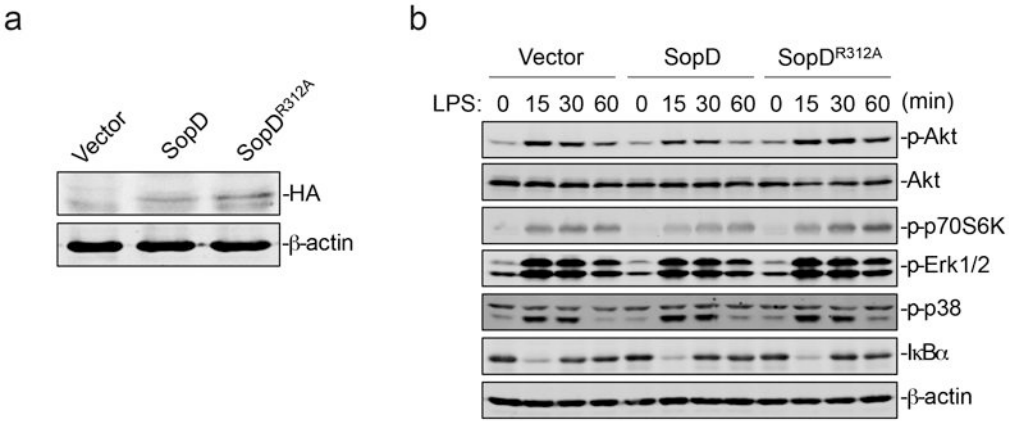

Extended Data Fig. 4. SopD enhances pro-inflammatory signaling by antagonizing Rab8 through its GAP activity.

(**a**) Expression levels of SopD and its catalytic mutant SopD^{R312A} in stable cell lines (Raw264.7). Stable cell lines (Raw264.7) expressing HA-tagged SopD or SopD^{R312A} were lysed before immunoblotting analysis with the antibodies directed to the HA tag and to β-

actin (as a loading control). (**b**) Effect of the expression of SopD or its catalytic mutant SopD^{R312A} on LPS-induced activation of AKT, p70S6K, Erk1/2, and p38 MAP, and NF-κB signaling pathways. Raw264.7 cells stably expressing HA-tagged SopD or its GAP-deficient mutant SopD^{R312A} were treated with LPS (100 ng/ml) for the indicated times, lysed, and analyzed by immunoblotting with antibodies specific for the phosphorylated state of AKT, p70S6K, p38, and Erk1/2, as well as an antibody to I-κBα and β-actin (as a loading control). The quantification of the western blot analyses is shown on Fig. 2e.

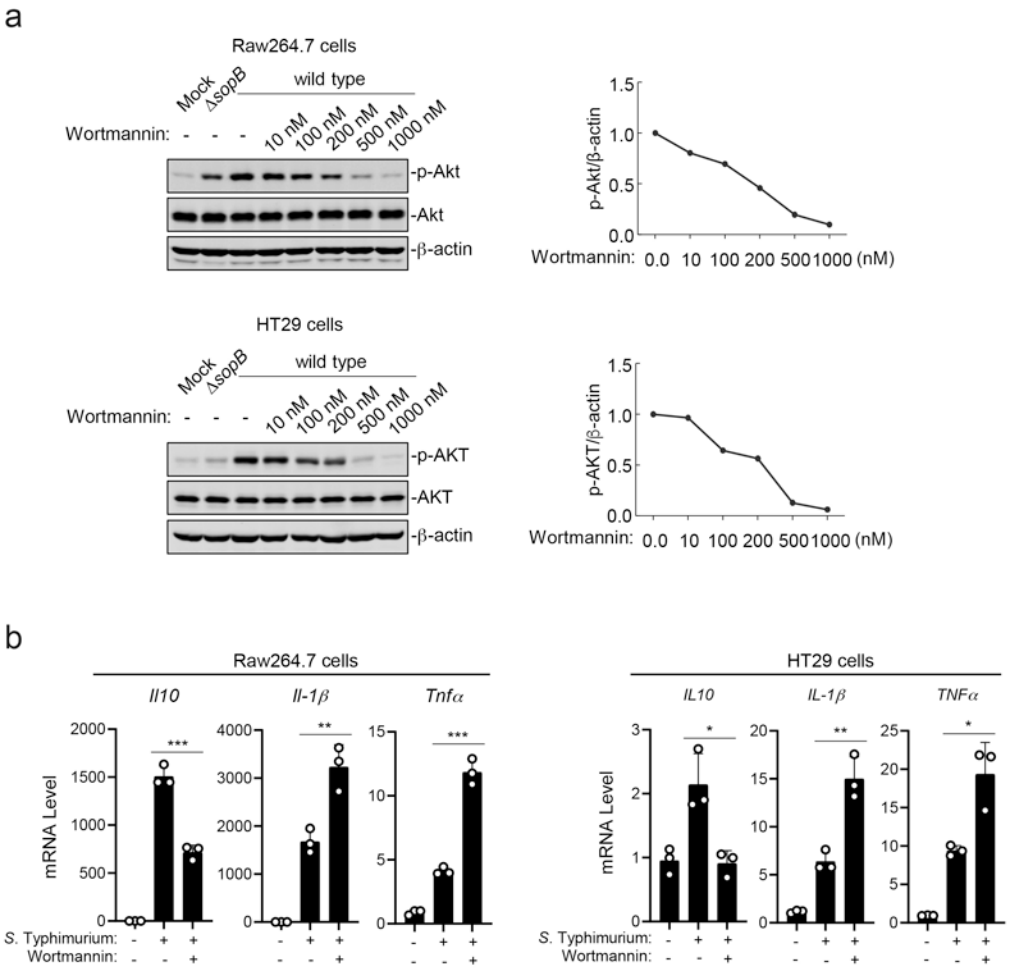

Extended Data Fig. 5. PI3-Kinase is required for *S*. Typhimurium-induced signaling.

(**a**) Effects of the PI3-Kinase inhibitor Wortmannin on *S*. Typhimurium-induced phosphorylation of AKT. Raw264.7 (MOI=2) or HT29 cells (MOI=10) were pre-treated with increasing concentrations of Wortmannin (10 nM to 1000 nM) for 30 min. Cells were then infected with wild-type *S*. Typhimurium for 30 min and cell lysates were analyzed by immunoblotting with antibodies directed to the phosphorylated (activated) form of Akt or β-actin (as a loading control). Controls included cells left uninfected or infected with the Δ*sopB S*. Typhimurium mutant strain, which is defective for the activation of AKT. Quantification of the immunoblots is shown on the right panels. (**b**) Effects of the PI3-Kinase inhibitor Wortmannin on *S*. Typhimurium-induced transcription of cytokine genes.

Raw264.7 cells (MOI=5) and HT29 cells (MOI=20) were pre-treated with Wortmannin (100 nM) for 30 min. Cells were left uninfected or infected with wild-type *S.* Typhimurium for 4 hs and the cytokine mRNA levels were measured by qPCR assay. In both, (**a**) and (**b**) data are the mean ± standard deviation of three independent experiments. ** $P < 0.01$, *** $P < 0.001$ (unpaired two-sided *t* test).

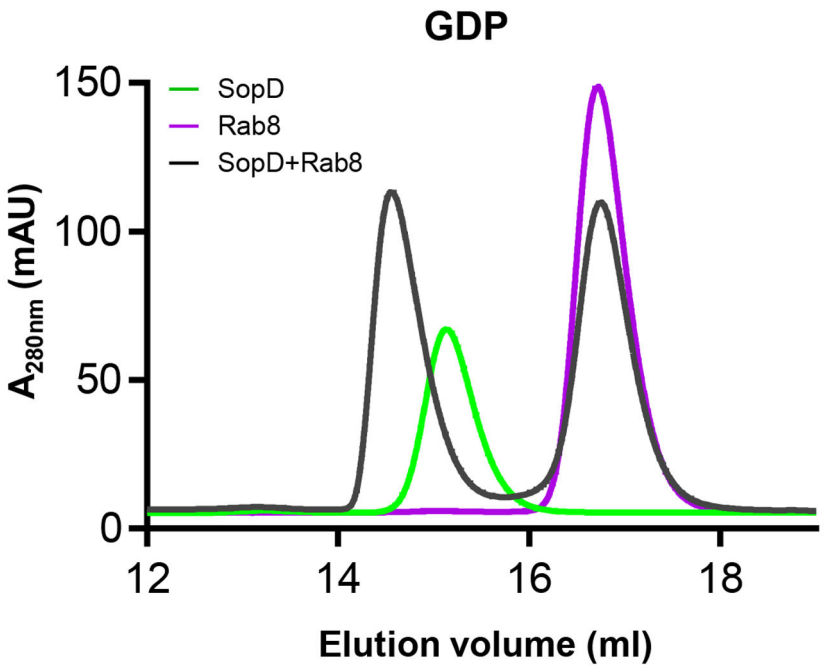

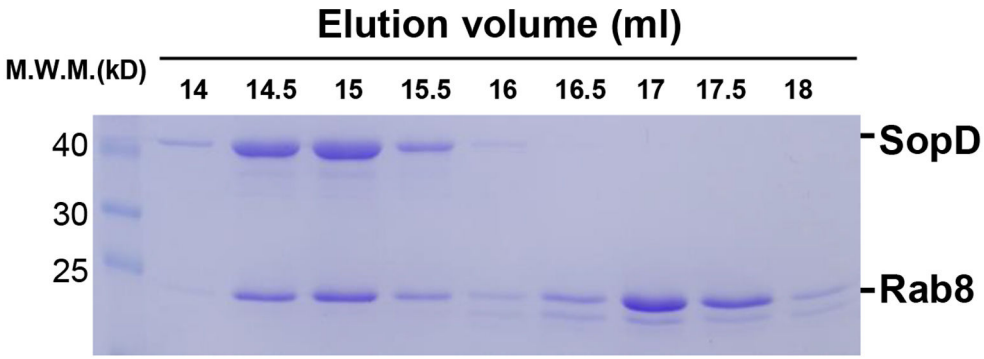

Extended Data Fig. 6. Size-exclusion chromatography profile of SopD/GDP-bound Rab8 complex.

Rab8$^{1-183}$ preloaded with GDP was incubated with SopD, and subjected to size-exclusion chromatography with Superdex 200 increase column. The elution profile along with the SDS-PAGE analyses of the elution fractions of the SopD/Rab8 complex are shown. This experiment was conducted at least three times with equivalent results.

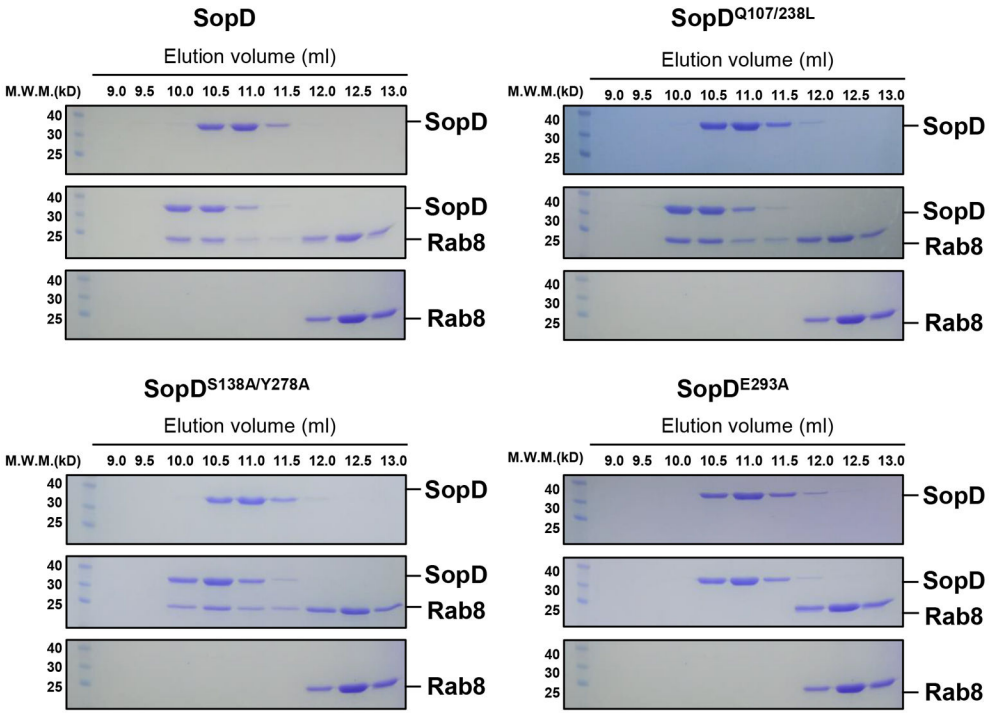

Extended Data Fig. 7. SDS-PAGE analyses of the elution fractions of the size-exclusion chromatography analyses of SopD carrying mutations in amino acids defining its interface with Rab8.

Purified Rab8a$^{1\text{-}183}$ preloaded with GDP was incubated with purified SopD or the indicated SopD mutants and subjected to size-exclusion chromatography (see the chromatographic profile in Fig. 3e). Fractions were collected, separated on an SDS-PAGE, and stained with Coomassie blue. This experiment was conducted at least three times with equivalent results.

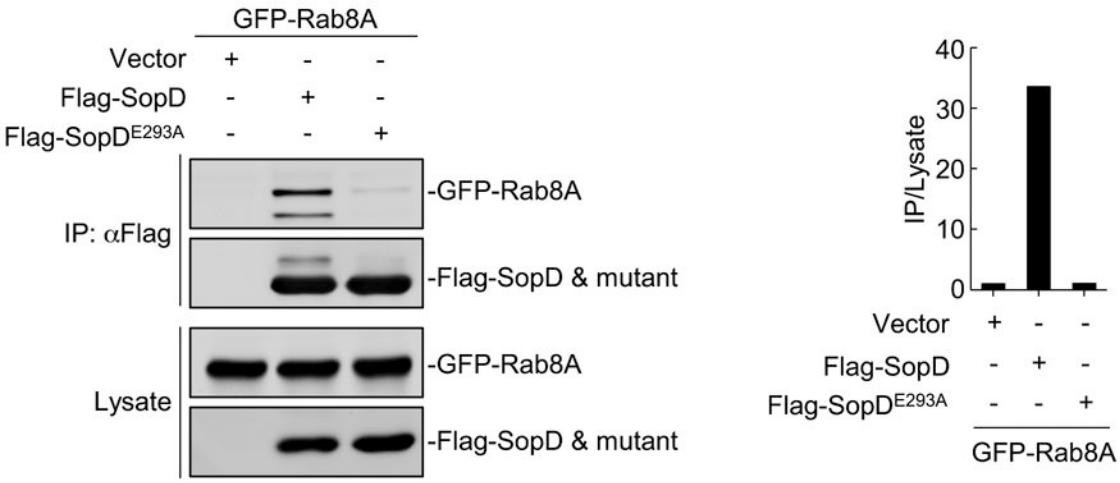

Extended Data Fig. 8. The SopD^{E293A} mutation disrupts the ability of SopD to form a complex with Rab8.

FLAG-epitope tagged SopD or SopD^{E293A} were co-expressed with GFP-Rab8 or empty vector in HEK-293T cells. The cell lysates were co-immunoprecipitated with anti-FLAG M2

beads followed by immunoblotting with anti-GFP and anti-Flag antibodies. The quantification of the intensity of the bands is shown in the right panel. This experiment was conducted at least three times with equivalent results.

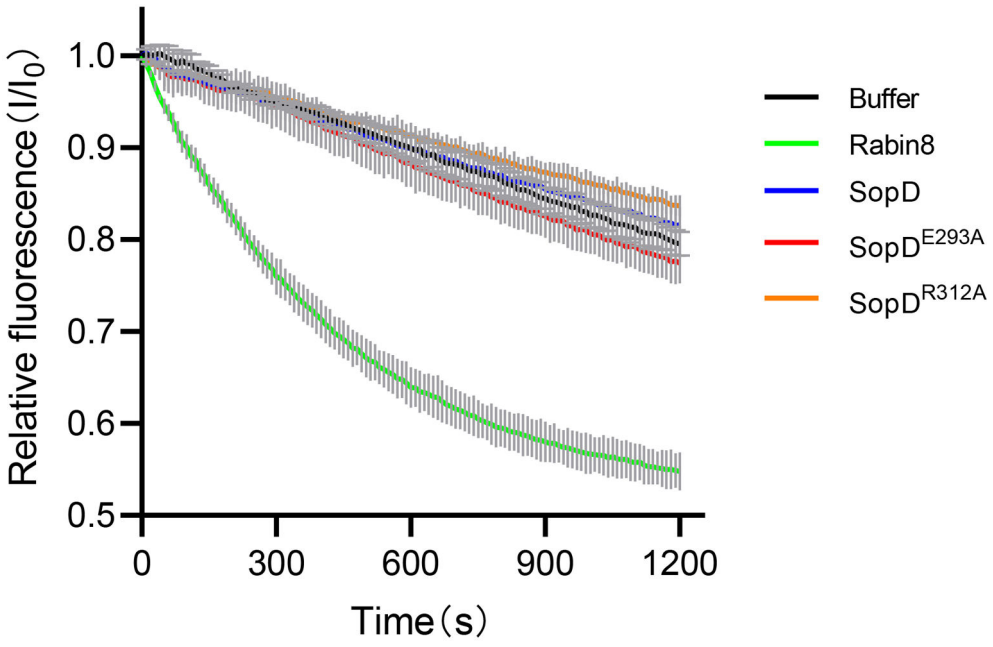

Extended Data Fig. 9. SopD lacks guanine-nucleotide exchange activity.

Mant-GDP-loaded Rab8a (2 μM) was incubated with Rabin8 (0.4 μM) (positive control), SopD (2 μM), 2 μM SopD^{R312A} (2 μM), SopD^{E293A} (2 μM) or buffer only (negative control), in the presence of 5 μM GTPγS. The decreased fluorescence as a result of the mant-GDP to GTPγS exchange was monitored over time. Data are expressed as the mean ± SD from three independent experiments.

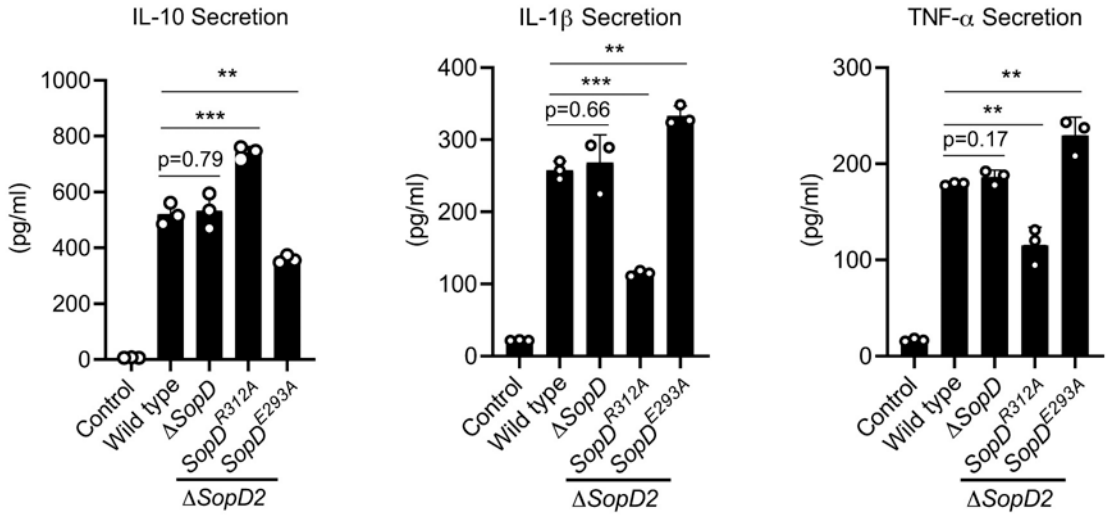

Extended Data Fig. 10. Effect of SopD or its mutants on cytokine production in *S*. Typhimurium-infected cells.

Raw264.7 cells were infected with the indicated *S.* Typhimurium strains (MOI=5) and 18 hours after infection, the levels of the indicated cytokines in cell supernatants were quantified by ELISA. Values are the mean ± SD of three independent measurements. ** $P < 0.01$, *** $P < 0.001$, ns: not significant $P > 0.05$ (unpaired two-sided *t* test).

Supplementary Material

Refer to Web version on PubMed Central for supplementary material.

ACKNOWLEDGEMENTS

We thank Dr. Jiawei Wang (Tsinghua University, China) for suggestions on structure date processing, the staff of the BL17U1 and BL19U1 beamlines of the National Facility for Protein Science Shanghai (NFPS) at Shanghai Synchrotron Radiation Facility (SSRF) for assistance during data collection, and Xiaoju Li (Shandong University, Core facilities for life and environmental sciences) for help with the XRD. Work in XG's laboratory was supported by the National Key R&D Program of China (2018YFE0113000), the National Natural Science Foundation of China (31770143 and 31901943), the Major Basic Program of Natural Science Foundation of Shandong Province (ZR2019ZD21), the Youth Interdisciplinary Innovative Research Group of Shandong University (2020QNQT009), and the Taishan Young Scholars Program (tsqn20161005). Work in JEG.'s laboratory was supported by NIH Grant R01AI055472 and R01AI079022.

References

1. Chen LM, Hobbie S & Galan JE Requirement of CDC42 for Salmonella-induced cytoskeletal and nuclear responses. Science 274, 2115–2118 (1996). [PubMed: 8953049]
2. Bruno VM et al. Salmonella Typhimurium type III secretion effectors stimulate innate immune responses in cultured epithelial cells. PLoS Pathog 5, e1000538, doi:10.1371/journal.ppat.1000538 (2009). [PubMed: 19662166]
3. Patel JC & Galán JE Differential activation and function of Rho GTPases during Salmonella-host cell interactions. J Cell Biol 175, 453–463, doi:10.1083/jcb.200605144 (2006). [PubMed: 17074883]
4. Sun H, Kamanova J, Lara-Tejero M & Galán JE Salmonella stimulates pro-inflammatory signalling through p21-activated kinases bypassing innate immune receptors. Nat Microbiol. 3, 1122–1130 (2018). [PubMed: 30224799]
5. Hobbie S, Chen LM, Davis R & Galán JE Involvement of the mitogen-activated protein kinase pathways in the nuclear responses and cytokine production induced by *Salmonella typhimurium* in cultured intestinal cells. J. Immunol 159, 5550–5559 (1997). [PubMed: 9548496]
6. Kamanova J, Sun H, Lara-Tejero M & Galán J The Salmonella Effector Protein SopA Modulates Innate Immune Responses by Targeting TRIM E3 Ligase Family Members. PLoS Pathog. 12, e1005552. (2016). [PubMed: 27058235]
7. Keestra A et al. A Salmonella virulence factor activates the NOD1/NOD2 signaling pathway. mBio 2, e00266–00211 (2011). [PubMed: 22186610]
8. Haraga A & Miller SI A Salmonella type III secretion effector interacts with the mammalian serine/threonine protein kinase PKN1. Cell Microbiol 8, 837–846 (2006). [PubMed: 16611232]
9. Stecher B et al. Salmonella enterica serovar typhimurium exploits inflammation to compete with the intestinal microbiota. PLoS Biol. 5, 2177–2189 (2007). [PubMed: 17760501]
10. Winter S et al. Gut inflammation provides a respiratory electron acceptor for Salmonella. Nature 467, 426–429 (2010). [PubMed: 20864996]
11. Fu Y & Galán JE A salmonella protein antagonizes Rac-1 and Cdc42 to mediate host-cell recovery after bacterial invasion. Nature 401, 293–297, doi:10.1038/45829 (1999). [PubMed: 10499590]
12. Sun H, Kamanova J, Lara-Tejero M & Galán J A Family of Salmonella Type III Secretion Effector Proteins Selectively Targets the NF-κB Signaling Pathway to Preserve Host Homeostasis. PLoS Pathog. 12, e1005484. (2016). [PubMed: 26933955]

13. Jones MA et al. Secreted effector proteins of Salmonella dublin act in concert to induce enteritis. Infection & Immunity 66, 5799–5804 (1998). [PubMed: 9826357]
14. Zhang S et al. The Salmonella enterica serotype typhimurium effector proteins SipA, SopA, SopB, SopD, and SopE2 act in concert to induce diarrhea in calves. Infect. Immun 70, 3843–3855 (2002). [PubMed: 12065528]
15. Wall A et al. Small GTPase Rab8a-recruited Phosphatidylinositol 3-Kinase γ Regulates Signaling and Cytokine Outputs from Endosomal Toll-like Receptors. J Biol Chem. 292, 4411–4422 (2017). [PubMed: 28130450]
16. Luo L et al. TLR Crosstalk Activates LRP1 to Recruit Rab8a and PI3Kγ for Suppression of Inflammatory Responses. Cell Rep. 24, Cell Rep. 2018 Sep 2011;2024(2011):3033–3044. (2018).
17. Tong S, Wall A, Hung Y, Luo L & Stow J Guanine nucleotide exchange factors activate Rab8a for Toll-like receptor signalling. Small GTPases 7, 1–17 (2019).
18. Brumell J et al. SopD2 is a novel type III secreted effector of Salmonella typhimurium that targets late endocytic compartments upon delivery into host cells. Traffic 4, 36–48 (2003). [PubMed: 12535274]
19. Spanò S, Gao X, Hannemann S, Lara-Tejero M & Galán J A Bacterial Pathogen Targets a Host Rab-Family GTPase Defense Pathway with a GAP. Cell Host Microbe 19, 216–226 (2016). [PubMed: 26867180]
20. Creagh E & O'Neill L TLRs, NLRs and RLRs: a trinity of pathogen sensors that co-operate in innate immunity. Trends Immunol. 27, 352–357 (2006). [PubMed: 16807108]
21. Lee J, Mo J, Shen C, Rucker A & Raz E Toll-like receptor signaling in intestinal epithelial cells contributes to colonic homoeostasis. Curr Opin Gastroenterol. 23, 27–31 (2007). [PubMed: 17133081]
22. Kelly D, Conway S & Aminov R Commensal gut bacteria: mechanisms of immune modulation. Trends Immunol. 26, 326–333 (2005). [PubMed: 15922949]
23. Eckmann L Sensor molecules in intestinal innate immunity against bacterial infections. Curr Opin Gastroenterol. 22, 95–101 (2006). [PubMed: 16462163]
24. Shibolet O & Podolsky D TLRs in the Gut. IV. Negative regulation of Toll-like receptors and intestinal homeostasis: addition by subtraction. Am J Physiol Gastrointest Liver Physiol. 292, G1469–1473 (2007). [PubMed: 17554134]
25. Lang T & Mansell A The negative regulation of Toll-like receptor and associated pathways Immunol Cell Biol. 85, 425–434 (2007). [PubMed: 17621314]
26. Hardt W-D, Chen L-M, Schuebel KE, Bustelo XR & Galán JE *Salmonella typhimurium* encodes an activator of Rho GTPases that induces membrane ruffling and nuclear responses in host cells. Cell 93, 815–826 (1998). [PubMed: 9630225]
27. Zhou D, Chen LM, Hernandez L, Shears SB & Galan JE A Salmonella inositol polyphosphatase acts in conjunction with other bacterial effectors to promote host cell actin cytoskeleton rearrangements and bacterial internalization. Mol Microbiol 39, 248–259 (2001). [PubMed: 11136447]
28. Sato T et al. Rab8a and Rab8b are essential for several apical transport pathways but insufficient for ciliogenesis. . J. Cell Sci 127, 422–431 (2014). [PubMed: 24213529]
29. Steele-Mortimer O et al. Activation of Akt/protein kinase B in epithelial cells by the Salmonella typhimurium effector sigD. J Biol Chem. 275, 37718–37724 (2000). [PubMed: 10978351]
30. Marcus S, Wenk M, Steele-Mortimer O & Finlay B A synaptojanin-homologous region of Salmonella typhimurium SigD is essential for inositol phosphatase activity and Akt activation. FEBS Lett. 494, 201–207 (2001). [PubMed: 11311241]
31. Pereira-Leal JB & Seabra MC The mammalian Rab family of small GTPases: definition of family and subfamily sequence motifs suggests a mechanism for functional specificity in the Ras superfamily. . J. Mol. Biol 301, 1077–1087 (2000). [PubMed: 10966806]
32. Pereira-Leal JB & Seabra MC Evolution of the Rab family of small GTP-binding proteins. J. Mol. Biol 313, 889–901 (2001). [PubMed: 11697911]
33. D'Costa V et al. Salmonella Disrupts Host Endocytic Trafficking by SopD2-Mediated Inhibition of Rab7. Cell Rep. 12, 1508–1518 (2015). [PubMed: 26299973]

34. Guo Z, Hou X, Goody RS & Itzen A Intermediates in the Guanine Nucleotide Exchange Reaction of Rab8 Protein Catalyzed by Guanine Nucleotide Exchange Factors Rabin8 and GRAB. J.Biol.Chem 288, 32466–32474 (2013). [PubMed: 24072714]
35. Hattula K, Furuhjelm J, Arffman A & Peränen J A Rab8-specific GDP/GTP exchange factor is involved in actin remodeling and polarized membrane transport. Mol Biol Cell. 13, 3268–3280 (2002). [PubMed: 12221131]
36. Homma Y & Fukuda M Rabin8 regulates neurite outgrowth in both GEF activity-dependent and -independent manners. Mol. Biol. Cell 27, 2107–2118 (2016). [PubMed: 27170183]
37. Müller M & Goody R Molecular control of Rab activity by GEFs, GAPs and GDI. Small GTPases. 2018 3 4;9(1-2):5–21. **9**, 5-21 (2018). [PubMed: 28055292] **9**
38. Cherfils J & Zeghouf M Regulation of small GTPases by GEFs, GAPs, and GDIs. Physiol Rev. 93, 269–309 (2013). [PubMed: 23303910]
39. Collins R "Getting it on"--GDI displacement and small GTPase membrane recruitment. Mol Cell. 12, 1064–1066 (2003). [PubMed: 14636566]
40. Sivars U, Aivazian D & Pfeffer S Yip3 catalyses the dissociation of endosomal Rab-GDI complexes. Nature 425, 856–859 (2003). [PubMed: 14574414]
41. Yamashita T & Tohyama M The p75 receptor acts as a displacement factor that releases Rho from Rho-GDI. Nat Neurosci. 6, 461–467 (2003). [PubMed: 12692556]
42. Hoiseth SK & Stocker BA Aromatic-dependent *Salmonella typhimurium* are non-virulent and effective as live vaccines. Nature 291, 238–239 (1981). [PubMed: 7015147]
43. Kaniga K, Bossio JC & Galan JE The Salmonella typhimurium invasion genes invF and invG encode homologues of the AraC and PulD family of proteins. Mol Microbiol 13, 555–568 (1994). [PubMed: 7997169]
44. Demarre G et al. A new family of mobilizable suicide plasmids based on broad host range R388 plasmid (IncW) and RP4 plasmid (IncPα) conjugative machineries and their cognate Escherichia coli host strains. Res. Microbiol. 156, 245–255 (2005). [PubMed: 15748991]
45. Gibson D et al. Enzymatic assembly of DNA molecules up to several hundred kilobases. Nat Methods. 6, 343–345 (2009). [PubMed: 19363495]
46. Kabsch W XDS. Acta Crystallogr D Biol Crystallogr. 66, 125–132. (2010). [PubMed: 20124692]
47. Collaborative Computational Project N The CCP4 suite: programs for protein crystallography. Acta Crystallogr D Biol Crystallogr. 50, 760–763 (1994). [PubMed: 15299374]
48. Emsley P & Cowtan K Coot: model-building tools for molecular graphics. Acta Crystallogr. D 60, 2126–2132 (2004).
49. Adams P et al. PHENIX: a comprehensive Python-based system for macromolecular structure solution. Acta Cryst. D66, 213–221 (2010).
50. DeLano WL The PyMOL Molecular Graphics System. http://www.pymol.org (2002).
51. Itzen A, Rak A & Goody R Sec2 is a highly efficient exchange factor for the Rab protein Sec4. J Mol Biol. 365, 1359–1367 (2007). [PubMed: 17134721]
52. Galán JE & Curtiss R III Cloning and molecular characterization of genes whose products allow *Salmonella typhimurium* to penetrate tissue culture cells. Proc. Natl. Acad. Sc. USA 86, 6383–6387 (1989). [PubMed: 2548211]
53. Chang S, Song J & Galán J Receptor-Mediated Sorting of Typhoid Toxin during Its Export from Salmonella Typhi-Infected Cells. Cell Host Microbe. 20, 682–689 (2016). [PubMed: 27832592]
54. Ran FA et al. Genome engineering using the CRISPR-Cas9 system. Nat Protoc 8, 2281–2308, doi:10.1038/nprot.2013.143 (2013). [PubMed: 24157548]
55. Lara-Tejero M et al. Role of the caspase-1 inflammasome in Salmonella typhimurium pathogenesis. J Exp Med 203, 1407–1412, doi:10.1084/jem.20060206 (2006). [PubMed: 16717117]

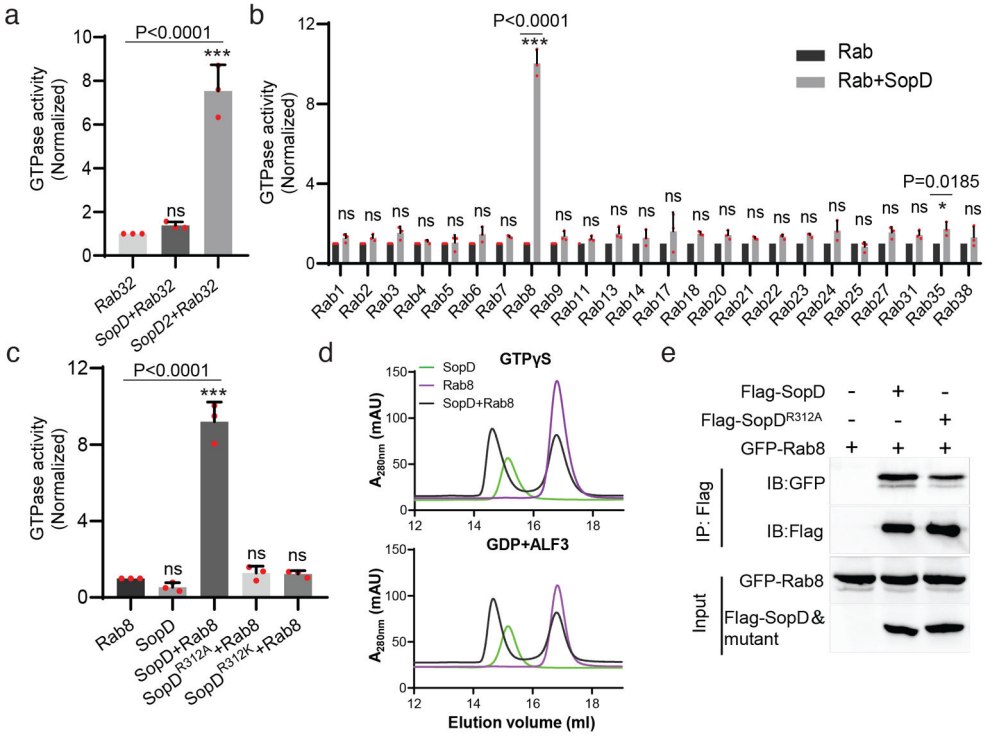

Figure 1. SopD is a GAP for Rab8.

(**a**) SopD lacks GAP activity toward Rab32. Purified Rab32 was incubated alone or in the presence of purified SopD or SopD2, as indicated, and the intrinsic GTPase activity was measured as indicated in Methods. (**b**) GAP activity of SopD toward Rab-family GTPases. Purified Rab GTPases were incubated alone or in the presence of purified SopD, and the intrinsic GTPase activity was measured as indicated in Methods. (**c**) SopD GAP activity toward Rab8 requires a critical arginine residue. Purified $Rab8^{1-183}$ was incubated alone or in the presence of purified SopD or the indicated mutants and the intrinsic GTPase activity was measured as indicated in Methods. Values in (**a**) (**b**) and (**c**) represent the ratio of GTPase activity observed in the presence or absence of SopD and are the mean ± SD from three independent experiments; ns, not significant; * $P < 0.05$, *** $P < 0.001$; n. s. $P > 0.05$ (**a** and **c**) one-way ANOVA with Dunnett's method, (**b**) Two-way ANOVA using Sidak's multiple comparisons test. (**d**) Size-exclusion chromatography profiles of SopD/Rab8 complex. $Rab8^{1-183}$ preloaded with GTPγS, or GDP+AlF_3 were incubated with SopD, and subsequently subjected to size-exclusion chromatography in a Superdex 200 increase column. (**e**) Co-immunoprecipitation to detect the interaction of SopD and $SopD^{R312A}$ with Rab8. HEK-293T cells were transiently co-transfected with plasmids expressing GFP-Rab8 along with plasmids expressing Flag-SopD, Flag-$SopD^{R312A}$ or the empty vector. Cell lysates were analyzed by co-immunoprecipitation with anti-Flag and western immunoblotting with anti-GFP and anti-Flag antibodies. Experiments in (**d**) and (**e**) were conducted at least three times with equivalent results.

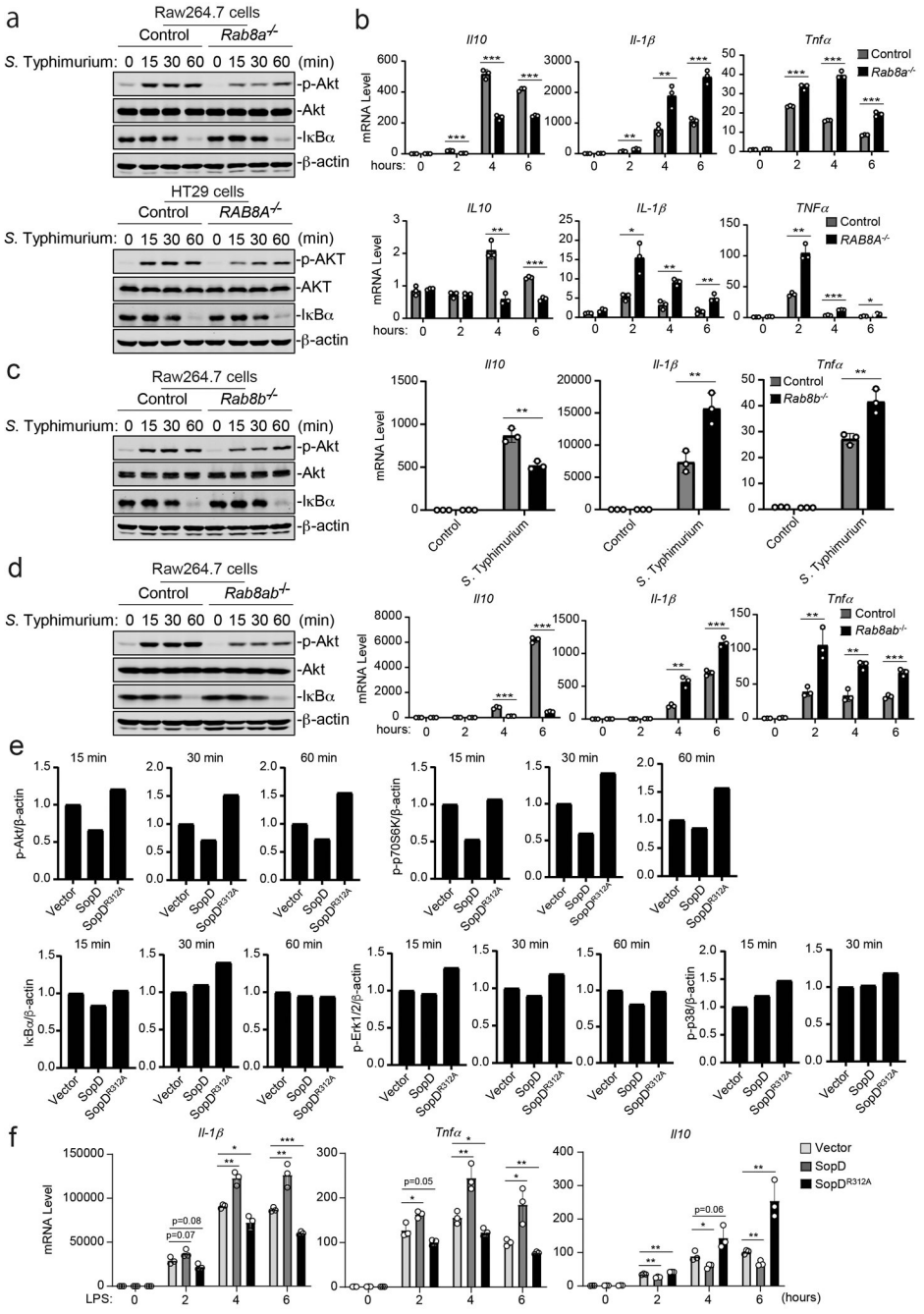

Figure 2. SopD enhances pro-inflammatory signaling by antagonizing Rab8 through its GAP activity.

(**a-d**) Effects of Rab8a or Rab8b deficiency on *S.* Typhimurium-induced Akt and NF-κB signaling. Control and Rab8a-, Rab8b-, or Rab8a/b-deficient Raw264.7 or HT29 (as indicated) cells were infected with wild-type *S.* Typhimurium with a multiplicity of infection of 2 and 10, respectively. At the indicated times after infection, the levels of phosphorylated AKT, the total levels of I-κBα, and the mRNA levels of the indicated cytokines were quantified by immunoblotting and qPCR. Values are the mean ± SD of three independent determinations. * $P < 0.05$, ** $P < 0.01$, *** $P < 0.001$, ns: not significant $P > 0.05$ (unpaired

two-sided *t* test). The quantification of the immunoblots is shown in Extended Data Fig. 3. (**e** and **f**) Effect of the expression of SopD or its catalytic mutant SopD^{R312A} on LPS-induced Akt, p70S6K, Erk1/2, p38 MAP, and NF-κB signaling and cytokine gene expression. Raw264.7 cells stably expressing HA-tagged SopD or its GAP-deficient mutant SopD^{R312A} were treated with LPS (100 ng/ml) for the indicated times, lysed, and analyzed by immunoblotting with antibodies specific for the phosphorylated state of Akt, p70S6K, p38, and Erk1/2, as well as an antibody to I-κBα and β-actin (as a loading control). The quantification of the western blot analyses is shown (**e**) A repetition of this experiment is shown in Supplementary Fig. 4. Values represent the mean ± SD of three independent determinations. * $P < 0.05$, ** $P < 0.01$, *** $P < 0.001$, ns: not significant $P > 0.05$ (unpaired two-sided *t* test). Alternatively (**f**), Raw264.7 cells stably expressing HA-tagged SopD or its GAP-deficient mutant SopD^{R312A} were treated with LPS (50 ng/ml) for the indicated times and the mRNA levels of the indicated cytokines were quantified by qPCR at the indicated times after treatment. Values are the mean ± SD of three independent determinations. * $P < 0.05$,** $P < 0.01$, *** $P < 0.001$, ns: not significant $P > 0.05$ (unpaired two-sided *t* test).

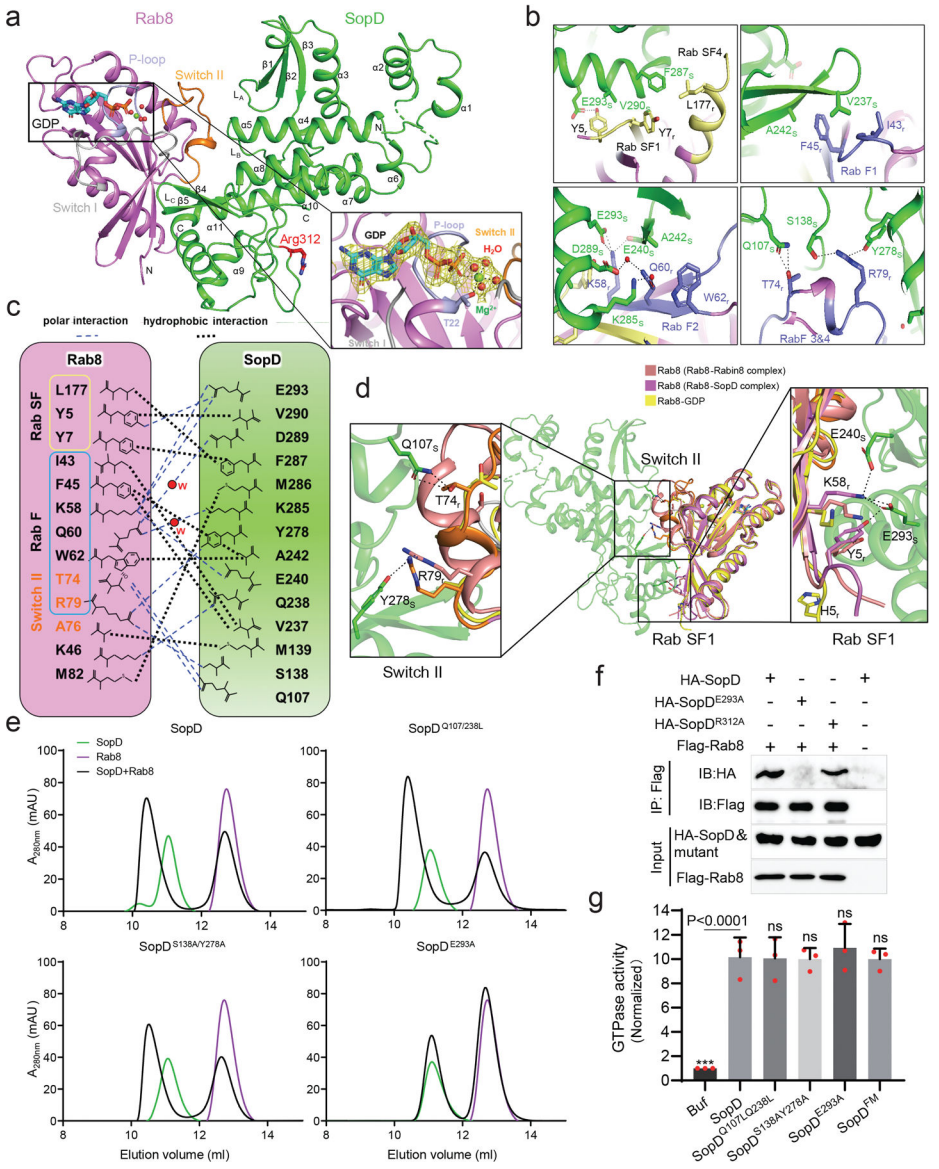

Figure 3. Crystal structure of the SopD/Rab8 complex and functional analyses of the binding interface.

(**a**) Ribbon representation of the overall structure of the SopD/Rab8 complex. The secondary structure features of SopD, as well as the position of the switch I (gray), switch II (orange), and P-loop (light blue) regions of Rab8 are indicated. The key catalytic residue arginine 312 in SopD is shown as stick and highlighted in red. The GDP is denoted as stick (cyan), water molecules and Mg^{2+} are represented as red and green spheres, respectively. The inset shows the simulated annealing omit maps (yellow mesh) for GDP, water molecules and Mg^{2+} in the nucleotide-binding pocket of Rab8 from the SopD/Rab8 complex (contoured at 1.5 **σ**). The T22 residue of Rab8, which forms a coordinate bond with Mg^{2+}, is shown as stick. (**b** and **c**) Depiction of the interactions between SopD (green) and Rab8 (violet) with interacting residues shown as sticks. RabSF and RabF motifs are depicted in yellow and light blue, respectively. Polar interactions are shown in black dashes. The schematic representation of

the interactions between Rab8 and SopD is shown in (**c**), where the polar interactions are shown as blue dashed lines, the water molecules as red balls, and the hydrophobic interactions as black dashed lines. (**d**) Structure superimposition of Rab8 as it appears in the Rab8/SopD complex, with Rab8 as it appears in complex with Rabin8 or bound to GDP. The inset shows the conformational changes of key amino acids in Rab8 after binding to SopD. (**e**) Size-exclusion chromatography analyses of SopD carrying mutations in amino acids defining its interface with Rab8. The SDS-PAGE analyses of the elution fractions are shown in Extended Data Fig. 7. (**f**) Co-immunoprecipitation analyses of the interaction of SopD and its indicated mutants with Rab8 after transient expression in HEK-293T cells. This experiment was conducted at least three times with equivalent results. (**g**) GAP activity of the indicated SopD mutants with substitutions in amino acid residues involved in its interface with Rab8. Data represent the ratio of GTPase activity observed in the presence or absence of SopD and are the mean ± SD from three independent experiments; ns, not significant $P > 0.05$; *** $P < 0.001$ (one-way ANOVA with Dunnett's method).

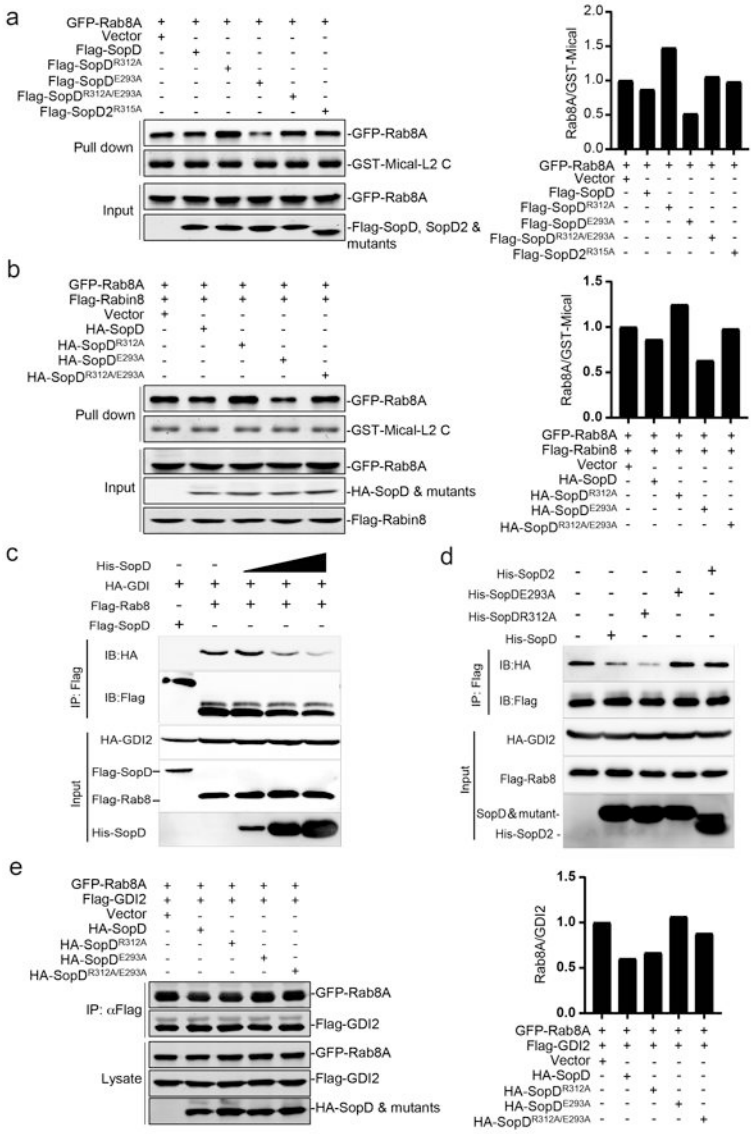

Figure 4. SopD activates Rab8 through a functional interface unrelated to its GAP activity.

(**a** and **b**) Effect of the transient expression of SopD^{R312A} (a GAP-defective mutant) or SopD^{E293A} (a mutant unable to form a complex with Rab8) on the levels of Rab8 activation. HEK-293T cells were transiently co-transfected with plasmids expressing wild-type SopD or the indicated mutants along with plasmids expressing GFP-tagged Rab8A (**a**) and, when indicated (**b**), Flag-tagged Rabin8, an exchange factor for Rab8a. Twenty hours after transfection, cells were lysed and the levels of GTP-loaded Rab8A were determined with the GST-Mical-L2 affinity probe as described in Methods. The quantification of the western blots is shown in the accompanying graphs. Values are represented relative to those obtained with vector control, which have been given the arbitrary value of 1. A repetition of this experiment is shown in Supplementary Fig. 9. (**c-e**) SopD displaces GDI2 from Rab8A. HEK-293T cells were co-transfected with plasmids expressing HA-tagged GDI2 and Flag-tagged Rab8. Twenty four hours after transfection, cells were lysed and 0.1, 0.5 or 1μg/ml of purified SopD (**c**), or 1μg/ml of purified SopD, SopD^{R312A}, SopD^{E293A}, or SopD2 (**d**) were

added to the cell lysates and the levels of Rab8a/GDI2 complex were determined by immunoprecipitation with anti-Flag antibody (directed to the tag in Rab8) and immunoblotting with an anti-HA antibody (directed to the tag in GDI2) (**c** and **d**). Alternatively (**e**), HEK-293T cells were transiently co-transfected with plasmids expressing GFP-tagged Rab8A and Flag-tagged GDI2, along with plasmids expressing the indicated HA-tagged SopD constructs. Twenty hours after transfection, cells were lysed and the levels of Rab8a/GDI2 complex were determined by immunoprecipitation with an anti-Flag antibody (directed to the tag in GDI2) and immunoblotting with an anti-GFP antibody (directed to the tag in Rab8A). The quantification of the western blots is shown in the accompanying graph. Values are represented relative to those obtained with vector control, which have been given the arbitrary value of 1. A repetition of this experiment is shown in Supplementary Fig. 9.

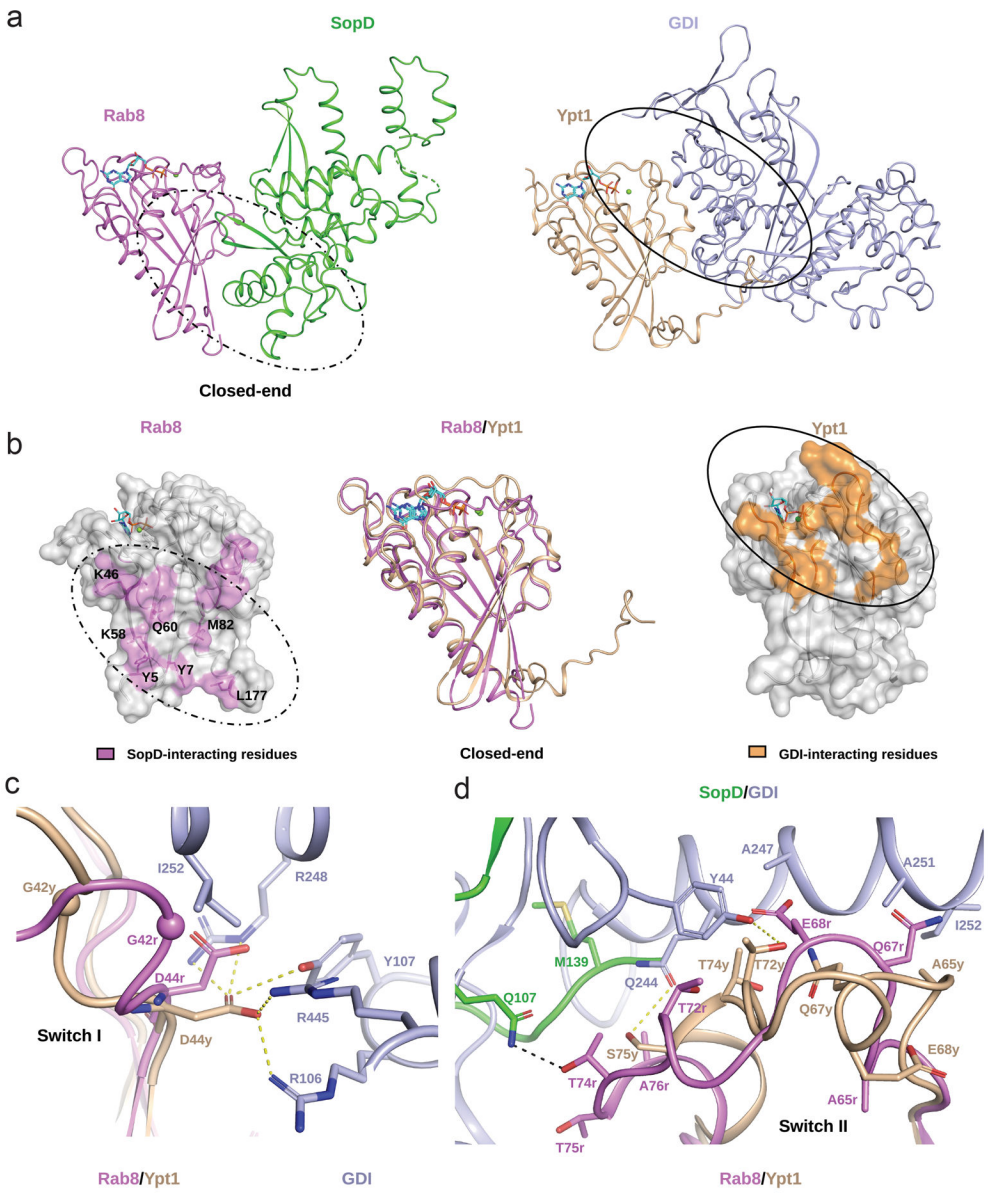

Figure 5. Structural basis for GDI displacement by SopD.

(**a**) Ribbon representation of the overall structure of the SopD/Rab8 and Ypt1/GDI (RCSB ID 2BCG) complex. (**b**) SopD and GDI bind to different surfaces on their cognate Rab GTPases. The residues of Rab8 and Ypt1 involved in their intermolecular interactions with SopD or GDI, respectively, are depicted on their surface structures in pink and orange, respectively (side panels). The structural alignment between Rab8 from the SopD/Rab8 complex structure and Ypt1 from GDI/Ypt1 complex are shown as ribbon in the central panel. The Rab8 amino acid residues specifically involved in its interaction with SopD at the "closed end" of Rab8/SopD complex are shown as sticks. In **(a)** and (**b**) GDP and Mg^{2+} bound to Rab8 or Ypt1 are represented as sticks and spheres, respectively. The interfaces between SopD/Rab8 and GDI/Ypt1 are highlighted with dotted and solid line circles, respectively. (**c** and **d**) SopD-induced conformational changes in switch I (**c**) and switch II

(**d**) of Rab8, highlighting residues involved in GDI-binding. Key interacting residues in Rab8 (G42r) and Ypt1 (G42y) are shown as ball representation. Other SopD-interacting residues involved in the GDI displacement process are shown as sticks. Hydrophobic interactions between Ypt1 and GDI and Rab8 and SopD are denoted by yellow and black dashed lines, respectively.

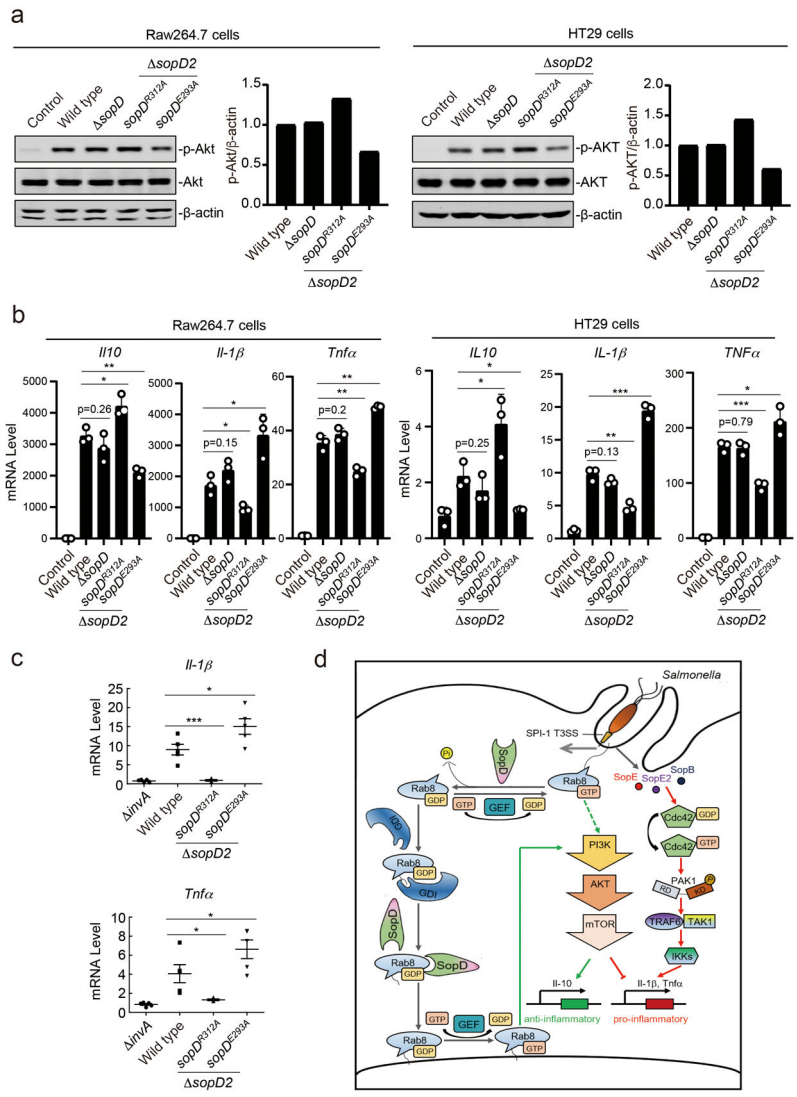

Figure 6. SopD positively and negatively modulates *S*. Typhimurium-induced inflammatory signaling through its independent Rab8-modulating activities.

(**a** and **b**) Akt activation and cytokine-gene expression in cells infected with *S*. Typhimurium strains expressing different *sopD* mutants. Raw264.7 (MOI=2) or HT29 (MOI=10) cells were infected with wild-type *S*. Typhimurium, the Δ*sopD* isogenic mutant, or the Δ*sopD2* mutant expressing the indicated mutant alleles of *sopD* for 60 minutes and Akt activation was analyzed by immunoblotting with antibodies specific for the phosphorylated state of Akt and β-actin (as a loading control). The quantification of the western blots is shown in the adjacent graphs. Values are represented relative to those obtained with wild type, which have been given the arbitrary value of 1. A repetition of this experiment is shown in Supplementary Figure 10. (**b**) Alternatively, Raw264.7 (MOI=5) or HT29 (MOI=20) cells were infected with the same *S*. Typhimurium strains (as indicated) and 4 hs after infection, the mRNA levels of the indicated cytokines were quantified by qPCR. Values represent fold induction relative to uninfected controls and are the mean ± SD of three independent determinations. * $P < 0.05$, ** $P < 0.01$, *** $P < 0.001$, ns: not significant $P > 0.05$ (unpaired

two-sided *t* test). (**c**) C57/BL6 *nramp*$^{+/+}$ mice (5 animals per strain) were orally infected (~1×10^{8} cfu) with wild-type *S.* Typhimurium, its isogenic Δ*invA* (type III secretion defective) mutant (as a negative control), or the *S.* Typhimurium Δ*sopD2* strains expressing the *sopD*^{R312A} or *sopD*^{E293A} alleles. Four days after infection the transcription levels of the indicated cytokine genes in the cells of the intestinal ceca were analyzed by qPCR assay. Values represent fold induction relative to animals infected with the *S.* Typhimurium Δ*invA* mutant strain and are the mean ± SD. * $P < 0.05$, *** $P < 0.001$ (unpaired two-sided *t* test). (**d**) Model for SopD action during *Salmonella* infection. *Salmonella* delivers T3SS effector proteins that activate membrane ruffling, inflammatory signaling, and the activation and recruitment Rab8 to the membrane ruffles. The GAP activity of SopD reverses the activation of Rab8 thus delaying or preventing Akt-dependent anti-inflammatory signaling. Later in infection, SopD stimulates Rab8 through its GDI-displacement activity leading to the stimulation of the anti-inflammatory program.